In presenting this dissertation as a partial fulfillment of the requirements for an advanced degree from the Georgia Institute of Technology, I agree that the Library of the Institute shall make it available for inspection and circulation in accordance with its regulations governing materials of this type.

I agree that permission to copy from, or to publish from, this dissertation may be granted by the professor under whose direction it was written, or, in his absence, by the Dean of the Graduate Division when such copying or publication is solely for scholarly purposes and does not involve potential financial gain.

It is understood that any copying from, or publication of, this dissertation which involves potential financial gain will not be allowed without written permission.

Richard Moran

LATERAL STABILITY OF BOX BEAMS SUBJECT TO PLASTIC MOMENT

A THESIS

Presented to

the Faculty of the Graduate Division

by

Richard Moran

In Partial Fulfillment

of the Requirements for the Degree

Master of Science in Civil Engineering

Georgia Institute of Technology

August, 1957

52
12R

LATERAL STABILITY OF BOX BEAMS SUBJECT TO PLASTIC MOMENT

Approved:

Dr. F. W. Schutz, Jr.

Dr. J. Mandelker

Prof. James R. Pincher

Date approved by Chairman: Aug 23, 1957

To my parents,

MR. & MRS. DEMETRIO MORAN

ACKNOWLEDGMENTS

The writer is deeply indebted to Dr. F. W. Schutz, Jr. for assistance throughout this investigation, for guidance and encouragement during both graduate and undergraduate studies, and for stimulating interest in the field of plastic analysis of steel structures.

Thanks are due Professor J. R. Fincher and Dr. J. Mandelker, members of the reading committee, for their assistance and recommendations.

I would like to thank the Atlantic Steel Company for the portion of the steel which they gratuitously supplied. Thanks are also due the Testing Division of the Georgia State Highway Department for performing the chemical analysis of the steel used in this study.

To Mr. C. M. Pavey of the Civil Engineering Department machine shop go thanks for the invaluable assistance in fabricating the test equipment.

TABLE OF CONTENTS

LIST OF TABLES

LIST OF FIGURES

LIST OF FIGURES (continued)

LIST OF SYMBOLS

a = width of flange overhang measured from center of web to free edge

b = distance between centers of web plates

c = total width of flange

d = depth of web

t_f = thickness of flange

t_w = thickness of web

Mp = plastic moment

My = moment corresponding to initial yield in the flanges

K = torsion constant analogous to the polar moment of inertia in the case of a round tube

Ixx = moment of inertia about the x-x axis

Iyy = moment of inertia about the y-y axis

L = length of beam test specimen, center to center of end pins

ℓ = length of compression test specimen

ϕ = unit rotation

ϕ_f = unit rotation at failure

ϕ_y = unit rotation at initial flange yield

ϵ_y = unit strain at yield point

ϵ_f = unit strain at local buckling

ϵ_{st} = unit strain at on-set of strain hardening

σ_{yu} = upper yield point

σ_y = lower yield point

LIST OF SYMBOLS (continued)

σ_{ult} = ultimate stress

σ_{cr} = stress at local buckling

E = Young's modulus of elasticity

Est = strain hardening modulus in a direction parallel to the loading

Ety = modulus in a direction perpendicular to loading (assumed to be the value E)

G = modulus of rigidity

G_{st} = modulus of rigidity in the strain hardening range

ν = Poisson's ratio (assumed to be 0.30 in all directions)

α = coefficient defining length of yielded zone at one end of compression member

k = nondimensional factor depending on the ratio of plate length to plate width and the edge conditions

SUMMARY

Due to the non-availability of adequate size standard rolled sections it frequently becomes necessary in practice to use built up sections. When such is the case, box sections, by virtue of their high torsional stiffness and bending stiffness in the lateral direction, provide a section which requires less bracing than the conventional I shape. Bracing requirements for box beams subject to plastic moment have not been established. The purpose of this investigation was to experimentally establish the critical length, as governed by lateral stability, of a given box section subject to plastic moment throughout its length.

A design chart was established for determining the most economical box section for use in plastically designed structures. The chart permits the selection of box sections on a basis of depth, plastic moment, area, or depth to width ratio. The chart was developed under the assumption that the material to be used was normal A-7 structural steel. The ratios of width to thickness of the components of the section were limiting values chosen to rule out local buckling in the plastic range.

Various lengths of the same cross section were tested by applying equal end moments to the specimens. No lateral buckling was observed. In all the tests, local buckling occurred in the plastic range prior to the onset of strain hardening.

Compression tests performed on short box sections verified the inadequacy of the previously established ratios of width to thickness

used to rule out the possibility of local buckling in the plastic range prior to the onset of strain hardening. The material used in fabricating the compression test specimens was the same material which was used in fabricating the beams. The premature local buckling encountered in this study was due to the low strain hardening modulus of the material. The results of coupon tension tests of the material used revealed a strain hardening modulus much lower than the average strain hardening modulus for A-7 structural steel.

Theoretical calculations are presented which reveal the intimate relationship between local buckling and the strain hardening modulus. Calculations of the width to thickness ratios required for the material used are also presented.

CHAPTER I

INTRODUCTION

One of the prime factors in plastic design is the adequate rotation of the plastic hinge. As a continuous mild steel structure is proportionally loaded some of the cross sections reach a specified moment and become plastified. Due to the ductile nature of mild structural steel these cross sections then rotate freely while maintaining a constant moment, a phenomenon called a "plastic hinge." The moment maintained by the plastic hinge, called the "plastic moment" of the cross section, is a function of the yield characteristics and geometry of the cross section. Further increase in load causes other cross sections subject to high moment to form plastic hinges while the original hinges undergo rotation, a process called "redistribution of moments." Redistribution of moments can occur only if the original hinges rotate without an appreciable increase in moment. When a sufficient number of hinges are formed to create a mechanism the structure collapses. Design of the structure is then based on the collapse load divided by an appropriate load factor.

If the cross sections in the areas of plastic hinge are weak in torsion and bending normal to the plane of loading, the section may buckle out of the plane of loading. If this lateral buckling occurs before adequate redistribution of moments is obtained, the predicted collapse load of the structure is not realized. In order to prevent

this type of premature failure the section must have adequate torsional strength and resistance to lateral bending. If the section is weak with respect to these characteristics it must be braced to insure rotation adequate for redistribution of moments.

The objective of the investigation was to experimentally establish the critical length, as governed by lateral stability, of a given box section subject to full plastic moment throughout its length. Adequate rotation to permit redistribution in most structures was assumed to be four times the rotation corresponding to initial yield in the flanges.

The experimental procedure was intended to provide a reasonable means of determining bracing requirements in areas of plastic hinge. The test is severe in that it requires the section to perform satisfactorily when the entire length is plastified. In most practical cases the area of plastic hinge is localized at a point of concentrated load.

A study was performed to find the most economical proportions of a box section to be used in plastically designed structures. The method used and the results of this study are presented in Appendix A. The limiting ratios of width to thickness used for proportioning the elements of the cross section were taken from tentative specifications for plastic design. These specifications are a result of experimental investigations on angles and wide flange beams performed at Lehigh University (1, 2).*

This investigation was limited to one size box section with unstiffened webs and no internal bracing.

---

*Numbers in parenthesis indicate references listed in the "Literature Cited" section of the bibliography.

CHAPTER II

DESCRIPTION OF TESTS

All test specimens were loaded in a RIEHLE Model PS-450, screw powered, constant strain testing machine with a capacity of 450 kips. Except where noted the strain rate was 0.025 inches per minute free head travel.

Beam Tests

Test Arrangement.--The general test arrangement is shown in Figs. 1 and 2. The loading beams were hung from the compression head of the testing machine by four 7/8 inch round bars and four 1/2 inch strap plates. A space of approximately 1/4 inch was left between the compression head and the loading beams to provide for differences in the initial camber of the beams. This space was filled with Leadite, a commercial compound used for capping concrete test cylinders. After the Leadite had hardened, the 7/8 inch round bars were tightened until the deflection of the strap plates was noticeable.

Each loading block consisted of a 10 inch length of 8WF67 beam with stiffeners. A surveying instrument was used to level the bottom faces of the loading blocks. Steel shims were used to insure bearing contact between the loading beams and the bearing blocks.

Each end block consisted of two pieces of 8WF17 beam welded to a lug plate. Vertical cross bracing of 1/2 inch round bar was welded between the beams at the bearing roller and midway from the bearing roller to the load roller. The distance between the bearing roller

and the load roller was kept constant for all the tests. This was done to keep the relationship between load and moment constant for all the test specimens.

The bearing blocks were each composed of two Tee sections cross braced with 1/4 inch round bars. The webs of the Tee sections were fastened to the bearing angles by means of high tensile bolts. This was done in such a manner as to cause the load to be transferred by friction between the Tee section web and the bearing angles. The bearing angles were tightly clamped to the spreader beams.

The spreader beams were cross braced vertically and horizontally at their ends and at the center, the cross bracing consisting of 1/2 inch round bars welded to the spreader beams.

The length of the specimens is given in Table 1. The cross section of the specimen is shown in Fig. 3.

Assembly of test specimens.--A core composed of aluminum and steel plates with a wood spacer board was used to maintain the desired distance between the webs of the test specimen. To provide for adjustment, the depth of the core was made approximately 1/2 inch less than the depth of the web plates. The web plates were clamped to the core and squared; the flange plates were then clamped to the web plates and centered. A continuous 1/8 inch fillet weld was placed at each exterior flange-web junction. After the specimen had cooled the core was removed and the specimen was butt welded to the face plates (the butt weld was continuous around the periphery of the section). The specimen was then placed in the loading apparatus. After each test the specimen was cut from the

face plates with an oxyacetylene torch. The face plates were then ground smooth and the process repeated for the next test.

Material.--The material used for the test specimens was taken from three hot rolled 11 gage steel sheets, 48 inches wide and 144 inches long. Coupons were cut in a lengthwise direction at 3 inch intervals across the width of the sheets. A number of coupons were tested from sheet number 2. This was done to establish the variation in physical properties across the sheet. The material used for the test specimens was cut lengthwise from the center portion of the sheet. Coupons tested from the center portions of sheets 1 and 4 gave the same results as those taken from the corresponding portion of sheet 2. The material used from sheets 1 and 4 was also cut from the center portion of the sheets.

Instrumentation.--A schematic drawing of the instrumentation used for the beam tests is shown in Fig. 4. The drawing is typical for all the beam tests with the exception of test B-1. The only instrumentation used for test B-1 is that shown at the centerline in Fig. 4.

The twist of the specimen was measured by the level indicator and twist bars shown in Fig. 5. The twist bars were attached to the top flange of the specimen by clamps. The double points of the level indicator were placed in the groove of the twist bar and the micrometer was adjusted until a level condition was indicated. The level indicator was then lifted from the twist bar and the micrometer reading taken. A general view of the centerline instrumentation is shown in Fig. 6.

Rotation was measured at the centerline as shown in Fig. 4. The slope bars clamped to the end blocks furnished a check on the rotation

measured at the centerline. The slope bars and the twist bars were identical. The level indicator was used as described previously to obtain readings from the slope bars.

A deflection truss hung from the bearing rollers served to refer the vertical deflection readings to the bearing rollers.

Horizontal deflection readings were taken at the centerline and at the face plates. The center horizontal reading was taken with the plunger of the micrometer dial gage bearing on the center of the web of the specimen. Readings at the face plates were taken with the plunger of the micrometer dial gage bearing on the edge of the face plate. The micrometer dial gages were mounted on stands which were clamped to the spreader beams.

Beam test procedure.--The same general procedure was used in all the beam tests. The apparatus was aligned and instrumentation placed on the specimen. The alignment was checked and bracing attached to hold the alignment. The bracing was removed and zero readings were taken at a load of 0.50 kips.

Test B-1 was loaded in 1 kip increments from the zero load to the expected flange yield load. Instrument readings were then taken at intervals governed by the amount of vertical deflection which had occurred. Tests B-2, B-3 and B-4 were loaded in 2 to 3 kip increments from zero to the flange yield load. Instrument readings were then taken at intervals governed by the amount of centerline twist and horizontal deflection which had occurred.

Test B-1.--The purpose of this test was to establish an experimental rotation curve for comparison with the theoretical curve. The length of the section was chosen to rule out any possibility of lateral buckling. The maximum load was 17.93 kips. At this point failure occurred by local buckling of the overhanging portion of the flange and adjacent web approximately 3-1/2 inches from the South face plate. General local buckling of a less pronounced nature was also observed in other areas of the flange overhang.

Test B-2.--The length of this section was the maximum that could be accomodated by the spreader beams. The maximum load was 18.0 kips. At 17.45 kips the centerline rotation dials were removed and the strain rate increased to 0.05 inches per minute free head travel. At 18.0 kips the strain rate was increased to 2.2 inches per minute. Local buckling of the flange overhang and adjacent web occurred 2 inches South of the centerline.

Test B-3.--The length chosen for this section was the maximum which could be accomodated by the loading beams. Longer spreader beams were obtained to replace those used in test B-2. Maximum load was 17.73 kips. At this load local buckling of the flange overhang and adjacent web was observed beneath the center twist bar. Twist readings of the center bar indicated that this local buckle began to form at a load of 17.25 kips. Local buckling of the specimen is shown in Fig. 7.

Test B-4.--The length of the specimen was chosen such that the depth to span ratio was approximately equal the maximum allowable depth to span

ratio given by the A.I.S.C. specifications. Extensions were placed on the loading beam to accomodate the specimen. At a load of 16.0 kips the horizontal deflection at the centerline began to increase at a greater rate than previously. This increase in horizontal deflection was not accompanied by any drop in load. The maximum load was 18.275 kips at which time local buckling of the flange overhang and adjacent web occurred abruptly 2 inches from the North face plate.

A general view of the test after failure may be seen in Fig. 8. The local buckling which occurred is shown in Fig. 9.

Compression Tests

General.--Direct compression tests were performed on short box sections to check the local buckling characteristics of the material used for making the beams. The method of assembly for the box sections was the same as that given for the beams. The material was taken from the center portion of sheet 2. The ratio of width to thickness for the web plates was made slightly less than the maximum permitted by the specifications (1, 2).

Instrumentation.--Instrumentation and specimen dimensions are shown in Figs. 10 and 11. In addition to the instrumentation shown in these figures, a micrometer dial gage was mounted on the base of the testing machine to measure the movement of the compression head of the testing machine.

Test C-1.--The load was applied in approximately 10 to 15 kip increments from zero to the expected yield load of 69 kips. At this point the load

was applied in 5 kip increments. Local buckling of the webs and adjacent flange overhangs occurred at a load of 75.0 kips. The local buckling was confined to the area approximately 1-1/2 inches from the top of the specimen.

Test C-2.--The specimen for this test was cut from the unbuckled portion of the specimen used in test C-1. The flange overhangs were cut from the specimen as shown in Fig. 11. The purpose of this test was to check the effect of the flange overhang on the critical strain of the webs. Local buckling of the webs occurred at a load of 64.8 kips. The local buckling was confined to an area 2 inches from the bottom of the specimen.

CHAPTER III

TEST RESULTS

Beam Tests

Rotation Curves.--Rotation curves for all the beam tests are shown in Figs. 12, 13, 14 and 15. A summary of the results is given in Table 2. All the test specimens displayed the assumed minimum required rotation. The theoretical rotation at initial yield was used in computing the ratio of the rotation at failure to the rotation at initial yield.

In all cases, the theoretical plastic moment agrees closely with the plastic moment observed in the tests. The departure of the test curves from the theoretical curve in the elastic range is due to local yielding of the flanges in the areas of residual strain caused by the welding.

In Figs. 13 and 14 the apparent discrepancy between the last readings of the rotation dials and the slope bars is due to the fact that the local buckle occurred within the gage length of the rotation dials. In all calculations the values of unit rotation used are those given by the rotation dials.

Horizontal deflection curves.--In all cases, minus (-) deflection represents deflection toward the West. The centerline deflections are given with respect to the ends of the specimen.

No horizontal deflection readings were taken in test B-1. The horizontal deflection curves for tests B-2 and B-3 are shown in Figs. 16

and 17. The curves for these tests give no indication of lateral buckling.

The specimen of test B-4 contained a noticeable initial curvature in the North half of the specimen. The effect of this curvature is evident in the horizontal deflection curve shown in Fig. 18. It is seen that as the specimen reached its full plastic moment, the deflection increased at a greater rate than in the elastic range. This behavior is associated with the loss in stiffness of the specimen upon plastification. The observed deflection was in the same direction as the initial curvature. No continued deflection was observed when loading was stopped to take readings. In spite of the effects of the initial curvature, the specimen reached the required rotation prior to local buckling.

Twist Curves.--The twist curves for all tests are shown in Figs. 19, 20, 21 and 22. Looking from South to North along the longitudinal centerline of the specimen, minus (-) twist is counterclockwise.

The apparent erratic nature of the curve for test B-1 is explained by the fact that only one twist bar was used. Therefore, all movements of the loading apparatus due to errors in alignment and leveling were recorded by the twist bar.

The twist curves for test B-2, B-3 and B-4 shown in Figs. 20, 21 and 22 show twist with respect to the ends of the specimen. The curves are not influenced by movements of the loading apparatus since twist bars 1 and 5 in Fig. 4, were used as reference for bars 2, 3 and 4. None of the above twist curves give any indication of lateral buckling.

Vertical deflection curves.--Figs. 23, 24, 25 and 26 show the vertical deflection curves for tests B-1, B-2, B-3 and B-4. The deflection curve for test B-1 is given with respect to the end rollers. The curves shown for tests B-2, B-3 and B-4 are given with respect to the ends of the specimen.

As in the case of the rotation curves, the deviation between the theoretical and test curves in the elastic range is due to localized yielding caused by residual strains in the areas adjacent to the welds.

Compression Tests

Tests C-1 and C-2.--The results of these tests are given in Table 3. The ratios used to guard against local buckling were intended to insure the attainment of strain hardening of the material prior to local buckling. This was not true in these tests. The results indicate that the ratios were unsatisfactory for the material used.

Material Properties

Coupons.--The results of the coupon tension tests are shown in Tables 4 and 5. A hydraulic testing machine with an electronic recorder was used to test the coupons in Table 4. A screw powered machine with a mechanical extensometer accurate to 0.0001 inches was used to test the coupons in Table 5. Due to the inaccuracy of the electronic recorder and the difficulty in maintaining a zero strain rate on the hydraulic machine, the values given in Table 5 are more accurate than those of Table 4. In all theoretical calculations the values used are an average of those given in Table 5.

Chemical analysis.--The results of a chemical analysis performed on the material used in these tests are shown in Table 6. The normal carbon content for mild structural steel of the A-7 type is in the order of 0.20 per cent. The chemical analysis revealed a carbon content of 0.036 per cent.

CHAPTER IV

THEORETICAL CONSIDERATIONS

No accurate theory with which to check the test results is available.

In Fig. 27 is shown a typical stress-strain curve for mild structural steel. Through the years many investigators have established theories which accurately describe the behavior of the material between point O and point A of the curve. Plastic design, however, is concerned with the portion of the curve from point A to point B. In this region the material has no apparent modulus of elasticity, though actually a modulus does exist. Yielding of mild steel takes place in small slip bands which begin to occur at points of stress concentration or weak areas in the crystalline structure of the material. After the first slip band has formed, slip bands begin to form throughout the material. If it were possible to measure the strain across these slip bands, it would be found that the strain "jumps" from point A to point C of the stress-strain curve as the slip occurs. This slipping is actually a rearrangement of the crystalline structure of the material. During the very short period of time required for this rearrangement the material may be thought of as having a modulus of zero. If a slip band occurs between two points from which strain readings are being taken, an elongation with no increase in load is noted. This behavior causes the flat portion of the curve between A and B. After the material has

generally undergone rearrangement of the crystals, the modulus becomes the strain hardening modulus.

The effective modulus of the material in the plastic range must be a function of the amount of apparent strain which has taken place and must always lie between the elastic modulus and the strain hardening modulus.

In a series of column tests performed on angles at Lehigh University by Thurlimann and Haaijer (3) the following behavior was observed: In the elastic range the average strain measured over the length of the member was equal to the strain measured at mid-length of the member. When the yield point of the material was reached the yielding was observed to take place at the ends of the specimen. The overall strain of the specimen increased while the strain at the mid-length of the member remained constant.

In their report, Thurlimann and Haaijer propose an approximate theory which in essence says that if buckling occurs, it must occur in the plastified regions at the ends of the column. The following assumptions are made in the theory:

1. The two end zones are yielded all the way to the strain hardening range. The middle zone is still elastic.

2. If buckling takes place, only the end zones will deform and the middle zone can be considered as rigid.

3. The yielded zones become anistropic such that the effective moduli become Est in the direction parallel to the loading, E in the direction perpendicular to the loading and the shearing modulus become $\sqrt{Est/E}\ G$. (3)

Thurlimann and Haaijer present the following formula for the outstanding leg of an angle:

$$\sigma_{cr} = \sigma_y = \frac{\pi^2 \, Est}{12(1 - \nu^2)} \left(\frac{t_f}{a}\right)^2 \left[\left(\frac{a}{\alpha \ell}\right)^2 + 0.425\right] * \qquad (1)$$

This is a modified form of the equation for the same case as given by Timoshenko (4). Thurlimann and Haaijer propose solving the above equation for α, the factor defining the yielded zones, and substituting its value in the following equation to obtain the critical strain:

$$\epsilon_f = (1 - 2\alpha)\,\epsilon_y + 2\alpha\,\epsilon_{st} \qquad (2)$$

In the case of tests C-1 and C-2, one unloaded edge of the flange overhang is free and the other unloaded edge is restrained. The true value of the critical strain must therefore lie between that given by Equation (1) and the value given by the equation for full fixity of the restrained edge. An approximate equation for the case of full fixity of the restrained edge is obtained by multiplying the right side of Equation (1) by the ratio of the "k" factors for the simply supported edge and the fixed edge conditions. Equation (1) then assumes the following form:

$$\sigma_{cr} = \sigma_y = \frac{\pi^2 \, Est}{12(1 - \nu^2)} \left(\frac{t_f}{a}\right)^2 \frac{1.277}{0.425} \left[\left(\frac{a}{\alpha \ell}\right)^2 + 0.425\right] \qquad (3)$$

The values of "k" used are those given by Bleich (5).

---

*The notation of this equation and subsequent equations has been modified to correspond with that of this study.

In the case of the web plates, Timoshenko (4) gives the following equation for the case of the unloaded edges simply supported;

$$\sigma_{cr} = \frac{\pi^2 E}{12(1 - \nu^2)} \left(\frac{t_w}{d}\right)^2 \left[\frac{d}{\ell} + \frac{\ell}{d}\right]^2 \qquad (4)$$

The formula is here modified by introducing the factor α and using Est. The resulting formula is as follows:

$$\sigma_{cr} = \sigma_y = \frac{\pi^2 Est}{12(1 - \nu^2)} \left(\frac{t_w}{d}\right)^2 \left[\frac{d}{\alpha\ell} + \frac{\alpha\ell}{d}\right]^2 \qquad (5)$$

In the case of full fixity of the unloaded edges, the right side of Equation (5) is multiplied by the ratio of the "k" factors as was done previously. Equation (5) then becomes:

$$\sigma_{cr} = \sigma_y = \frac{\pi^2 Est}{12(1 - \nu^2)} \left(\frac{t_w}{d}\right)^2 \frac{6.97}{4.00} \left[\frac{d}{\alpha\ell} + \frac{\alpha\ell}{d}\right]^2 \qquad (6)$$

In each case the critical strain is determined by using Equation (2). The above equations were used to determine the critical strains of the flange overhang and web plates of the specimens in tests C-1 and C-2. Results of these calculations are given in Table 7.

The following equations have been derived at Lehigh University (2) for the purpose of defining the stability of plates in the strain hardening range. The equations are based on a uniform load applied to two opposite edges of the plate. The loaded edges are simply supported in all cases. The following are the equations given for various conditions of restraint of the unloaded edges:

One unloaded edge free and the other simply supported:

$$\sigma_{cr} = \left(\frac{t_f}{a}\right)^2 \quad G_{st} \tag{8}$$

One unloaded edge free and the other fixed:

$$\sigma_{cr} = \left(\frac{t_f}{a}\right)^2 \left[\frac{7.275 \sqrt{Est\ Ety} - 0.506(\nu_y\ Est + \nu_x\ Ety)}{12(1 - \nu_x \nu_y)} + 1.371\ G_{st}\right] \tag{9}$$

Both unloaded edges simply supported:

$$\sigma_{cr} = \frac{\pi^2}{12} \left(\frac{t_w}{d}\right)^2 \left[\frac{\sqrt{Est\ Ety} + \nu_y\ Est + \nu_x\ Ety}{1 - \nu_x\ \nu_y} \quad 4\ G_{st}\right] \tag{10}$$

Both unloaded edges fixed:

$$\sigma_{cr} = \frac{\pi^2}{12} \left(\frac{t_w}{d}\right)^2 \left[\frac{4.554 \sqrt{Est\ Ety} \quad 1.237(\nu_y\ Est + \nu_x\ Ety)}{1 - \nu_x\ \nu_y} \quad 4.943\ G_{st}\right] \tag{11}$$

The above equations may be solved for the ratio of width to thickness which will permit the plate to reach the onset of strain hardening. This is done by substituting the values of the physical properties which correspond to the strain hardening range into the above equations. The yield stress of the material is substituted for the critical stress. The results of such calculations for the material of this study are given in Table 8. The value of G_{st} used in these calculations is the average of

that for A-7 steel reduced in proportion to the ratio of the average strain hardening moduli of A-7 steel and the material of this study. Ratios given by the tentative specifications are based on simply supported edges. Inspection of Table 8 shows that the ratios should have been smaller to insure the attainment of strain hardening for the material used in this study.

No attempt is made to develop an equation which describes the lateral stability of the beams in question. The development of such an equation is beyond the scope of this study.

Some idea of the lateral stability characteristics of the box section used in the tests may be obtained by substituting into the following equation given by Timoshenko (6):

$$Mcr = \frac{\pi \sqrt{EI_{yy} KG}}{L} \qquad (7)$$

This equation describes the elastic stability of a narrow rectangular strip subject to equal and opposite end moments. The ends are assumed to be simply supported and restrained against twist and movement in the horizontal direction. Using the proper values for the box section in question and taking Mcr as the moment corresponding to initial flange yield a solution for the critical length gives 83.2 feet. This is a conservative estimate since the proper magnification factor to account for the increased torsional resistance due to bending of the flanges and webs has not been applied to Equation (7).

Any attempt to develop an equation describing the lateral stability of the beam in the plastic range must account for different values of E

within the section at successive amounts of rotation in the plastic range. The large deflection in the plane of loading must also be taken into consideration.

CHAPTER V

DISCUSSION AND CONCLUSIONS

The required rotation capacity of a plastic hinge varies with the location of the hinge and the dimensions of the structure. To cover all possibilities, it is commonly assumed that the rotation capacity should be such that the hinge reaches strain hardening. This requirement is unnecessary, since the rotation capacity for any given hinge may be calculated. The criteria for adequate rotation capacity given in the Introduction is arbitrary and assumes that there is good agreement between the theoretical moment-rotation curve and the actual curve in the elastic range. Prediction of the collapse load is based on hinge rotation at its plastic moment value.

In the tests performed, the full plastic moment of the section was reached only shortly before failure by local buckling. Such performance would have been unacceptable in a structure where a hinge rotation capacity of four was required. There are two reasons for the poor performance of the test specimens. The first and most important of these is the low strain hardening modulus of the material used. As was mentioned in Chapter I, the ratios of the width to thickness used in designing the component parts of the cross section resulted from investigations performed on angles and wide flange beams of normal A-7 structural steel. These ratios are intended to insure the attainment of strain hardening of the material prior to local buckling. Inspection

of the properties of the material used in the Lehigh tests (2, 3), reveals a strain hardening modulus that varies from approximately 500 kips per square inch to 1100 kips per square inch. A large number of tension tests performed on A-7 steel at the same institution give an average value for the strain hardening modulus of 900 kips per square inch (1). In no case was the strain hardening modulus as low as that for the material used in this study. For A-7 steel an average value of the ratio of the ultimate stress to the yield stress is 1.9. The average value for the ratio of the ultimate stress to the yield stress was 1.3 for the material used in making the test specimens. By examining Equation (1) of Chapter IV, it may be seen that the strain hardening modulus is one of the dominant factors in determining stability in the plastic range. The second reason for the poor performance of the specimens of these tests is the effect of welding. In reality, this effect would have been of minor consequence had the local buckling not occurred. The premature yielding which took place in the elastic range retarded the development of the full plastic moment thus decreasing the amount of rotation which took place at the plastic moment value prior to local buckling.

The material obtained for these tests was not representative of a normal A-7 structural steel. Evidence of this fact is the very low carbon content revealed by the chemical analysis. The average values of lower yield stress and ultimate stress were 40 kips per square inch and 50 kips per square inch respectively. The probability of obtaining A-7 steel with a strain hardening modulus as low as that found in the material used in these tests is remote.

In considering the effect of welding in the case of built up sections, it should be borne in mind that the tests of this study were at model scale. In practice, heavier plates would be used and the size of the welds with respect to the plate dimensions would be such that the effects of residual strains in the areas of welding would be negligible.

In comparing the compression test results to the theoretical calculations it should be noted that local buckling was detected by visual observation only. It is possible that the inception of local buckling occurred at a unit strain lower than that given by the test results.

The only definite conclusions that may be drawn from the tests of this investigation is that local buckling in the plastic range is intimately related to the strain hardening modulus of the material.

CHAPTER VI

RECOMMENDATIONS

1. In choosing material to be used in plastic design, proper attention should be given the ratio of the ultimate stress to yield stress. Since the elongation at ultimate load is approximately the same for all mild structural steel, this ratio will give an indication of a low strain hardening modulus. For A-7 structural steel this ratio is approximately 1.9.

2. A series of tests similar to those of this thesis should be performed to establish the critical length of slender box beams. Material whose properties are consistent with those of A-7 steel should be used. It is suggested that the initial test of this series be performed on a specimen of the same length as that used in test B-4 of this study.

3. After the critical length for the slender box section is established, tests should be performed on box sections having a smaller depth to width ratio to establish a rule for the critical length of box sections. Design rules for bracing requirements in areas of plastic hinge could then be developed from the test results.

4. The behavior of the knees of rigid frames made of box sections should be investigated.

5. In any case in practice where it is necessary to resort to a built up section, the possibility of using a box section should not be

overlooked. The reduction in the amount of bracing required due to the good lateral stability characteristics of the box section results in economy and improves the aesthetic value of the structure.

APPENDIX A

DETERMINATION OF MOST ECONOMICAL BOX SECTION

DETERMINATION OF MOST ECONOMICAL BOX SECTION

The general cross section is as shown in Fig. 28.

The tentative specifications (1, 2) give the following ratios for the component parts of the cross section:

$$\frac{a}{t_f} \leq 8$$

$$\frac{b}{t_f} \leq 34$$

$$\frac{d}{t_w} \leq 50$$

This study is based on the following ratios:

$$\frac{a}{t_f} = 8 \qquad \text{(a)}$$

$$\frac{b}{t_f} = 34 \qquad \text{(b)}$$

$$\frac{d}{t_w} = 50 \qquad \text{(c)}$$

$$c = 50t_f \qquad \text{(d)}$$

The general expression for the plastic moment is:

$$M_p = \sigma_y \left[t_w \frac{d^2}{2} + (d + t_f)\, ct_f \right] \qquad \text{(e)}$$

Substituting Equations (c) and (d) into Equation (e) and simplifying the following equation results:

$$Mp = 50\sigma_y \left[25t_w^3 + 50t_w t_f^2 + t_f^3 \right] \qquad (f)$$

The general expression for the total area of the section is as follows:

$$A = 100 \left[t_f^2 + t_w^2 \right] \qquad (g)$$

In Fig. 2 Equations (f) and (g) are plotted as contours. The abscissa and ordinate scales are given in standard plate sizes. Several d/b ratios are also plotted in Fig. 2. The plot is used by following the curve for the plastic moment desired and choosing the plate sizes that correspond to the minimum area for the desired plastic moment. It should be noted that the curves for plastic moment and area are relatively insensitive to changes in d/b for sections with a d/b ratio of greater than 2. This indicates that no appreciable economy results by using a slender section.

The tests were to be at model scale. The smallest plate size considered convenient for fabrication was 1/8 inch. On this basis the section shown in Fig. 3 was chosen for the tests.

APPENDIX B

FIGURES

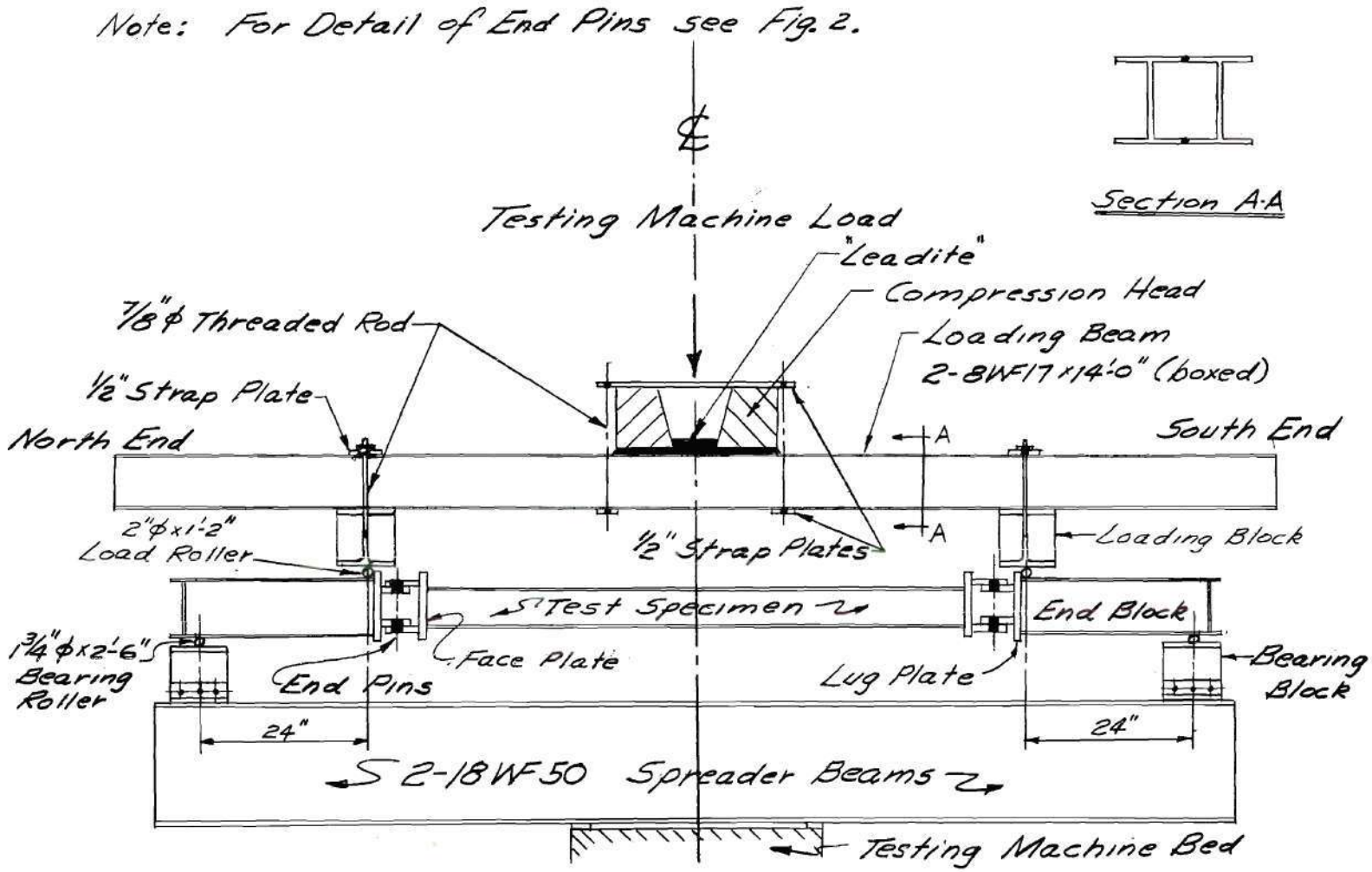

Fig. 1. General Test Arrangement for Beam Tests

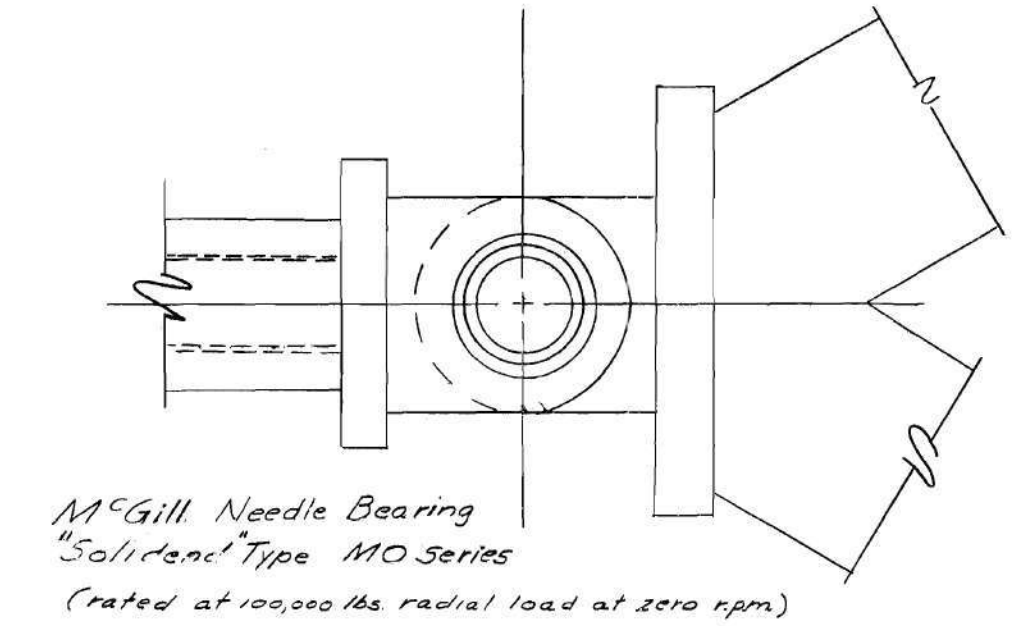

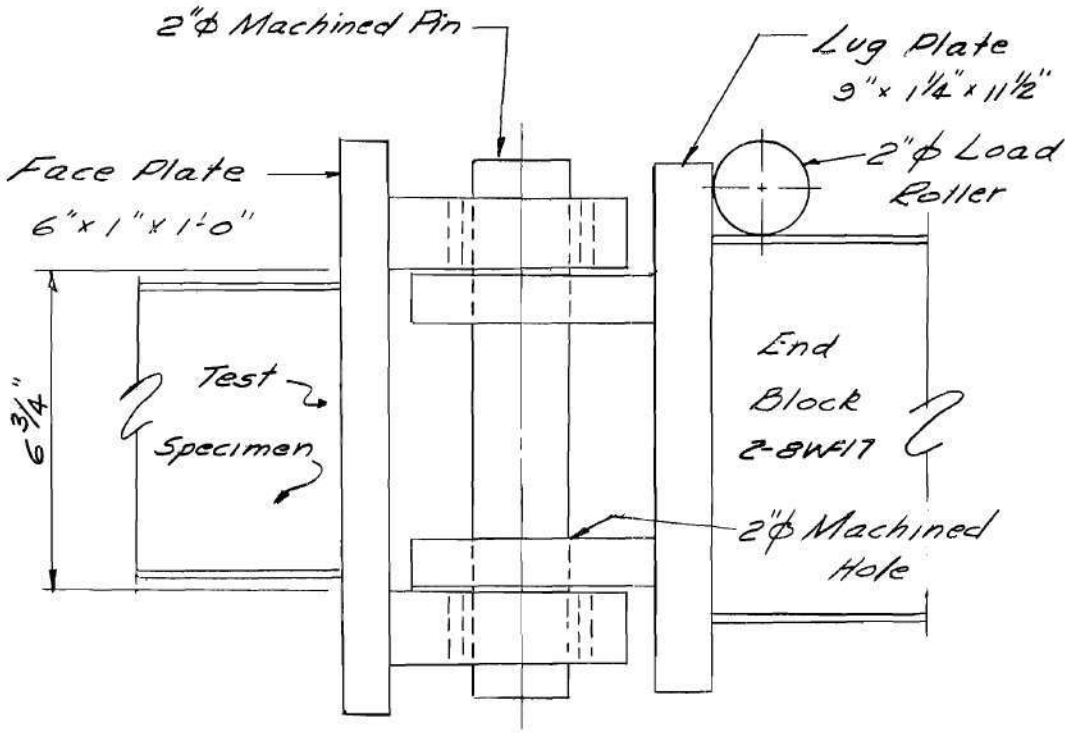

Fig. 2. Detail of End Pin

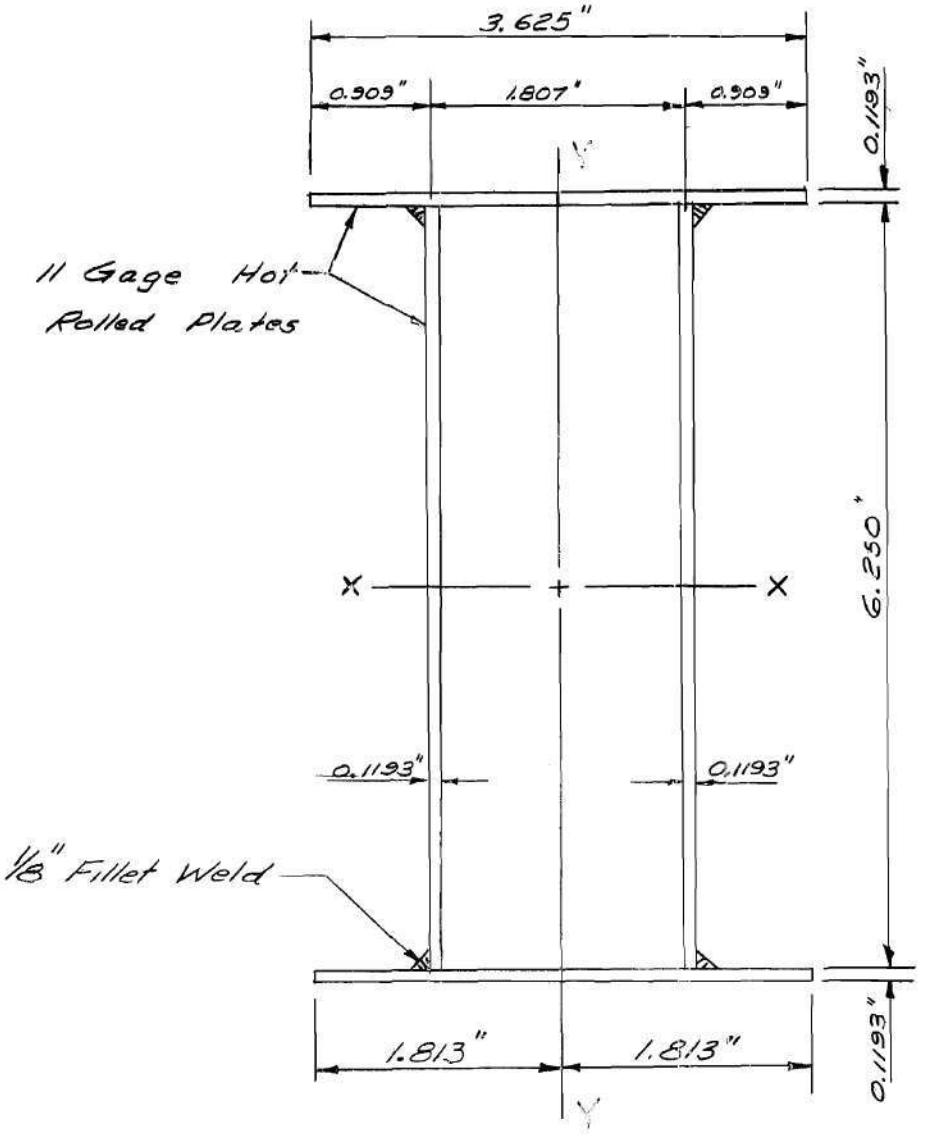

$\frac{a}{t_f}$ = 7.60

$\frac{b}{t_f}$ = 15.1

$\frac{d}{t_w}$ = 52.3

$\frac{d}{b}$ = 3.46

Mp = 207.3 kip-inches

My = 172.0 kip-inches

K = 3.86 $in.^4$

I_{xx} = 13.94 $in.^4$

I_{yy} = 2.08 $in.^4$

Area = 2.39 $in.^2$

Fig. 3. Cross Section and Properties of Test Specimens

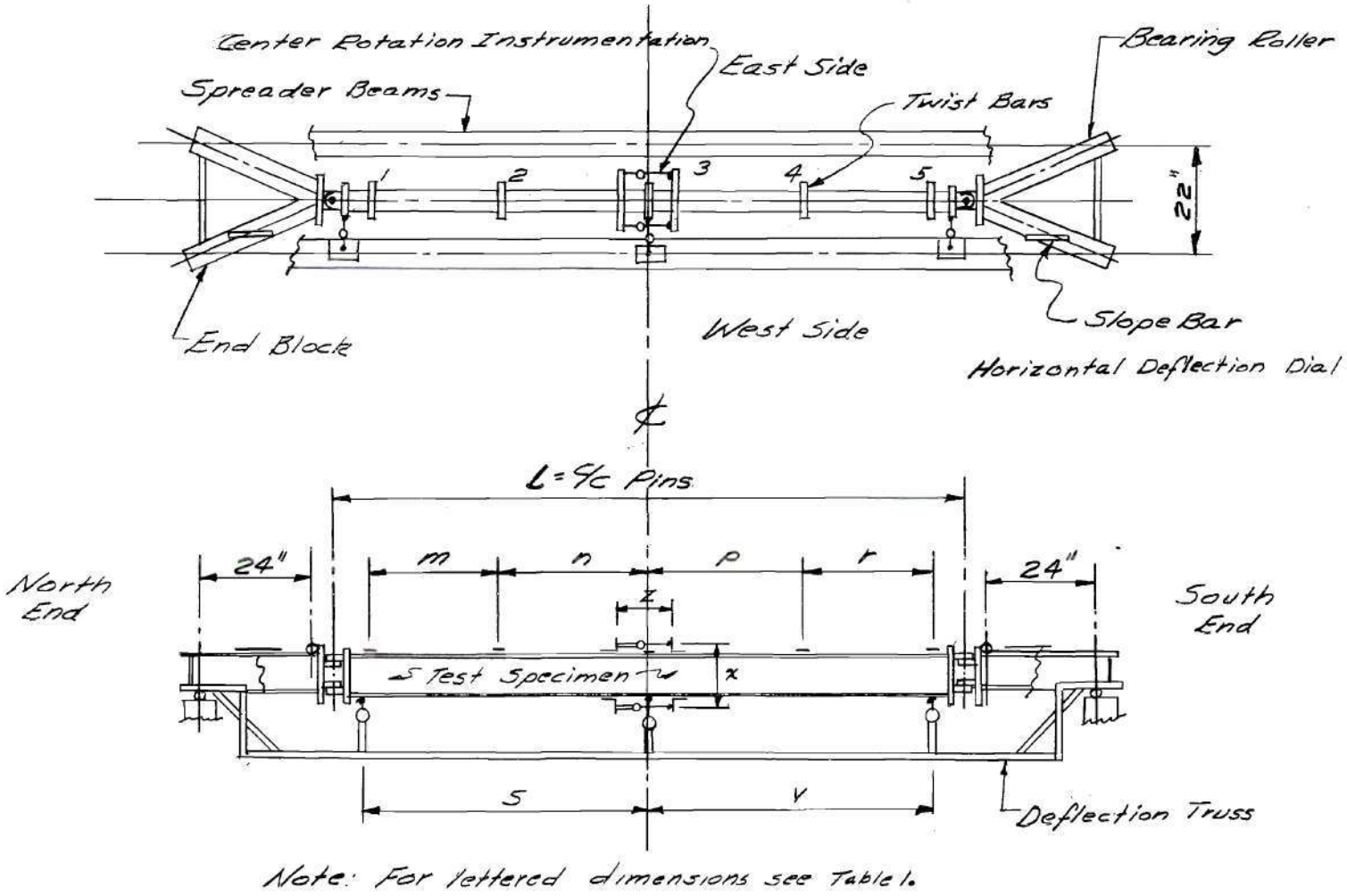

Note: For lettered dimensions see Table I.

Fig. 4. Schematic Drawing of Instrumentation

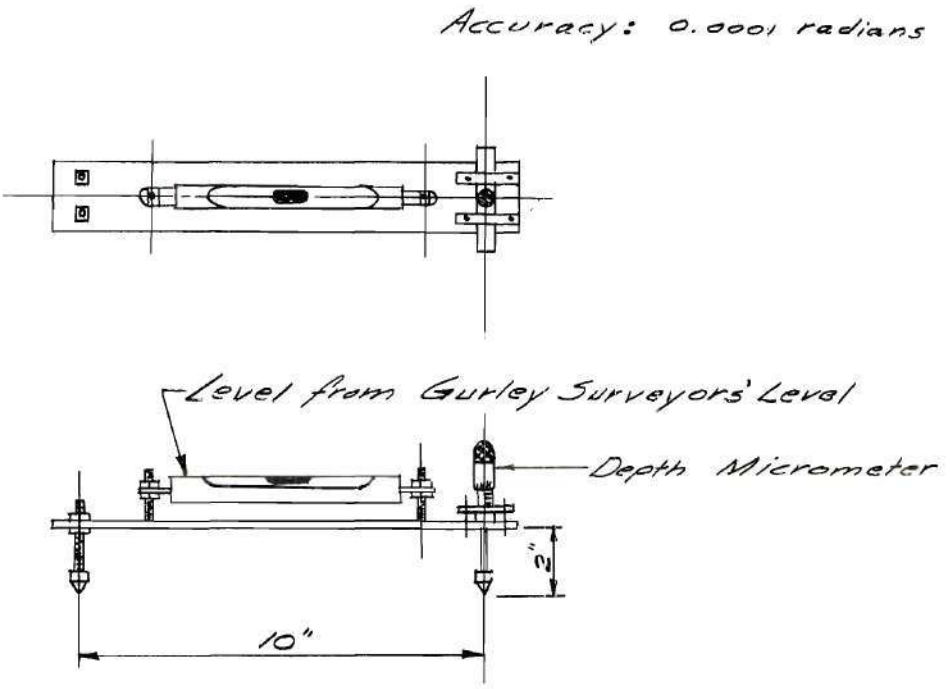

Level Indicator

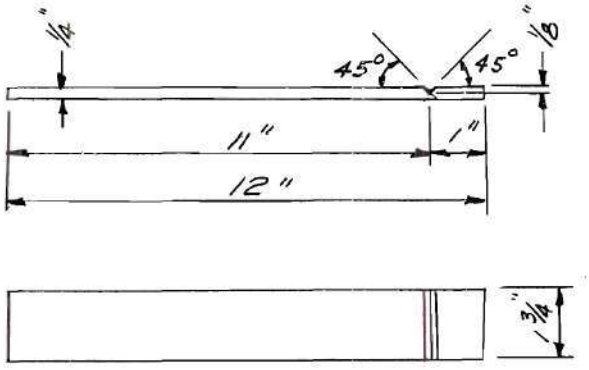

Twist Bar

Fig. 5. Details of Level Indicator and Twist Bars

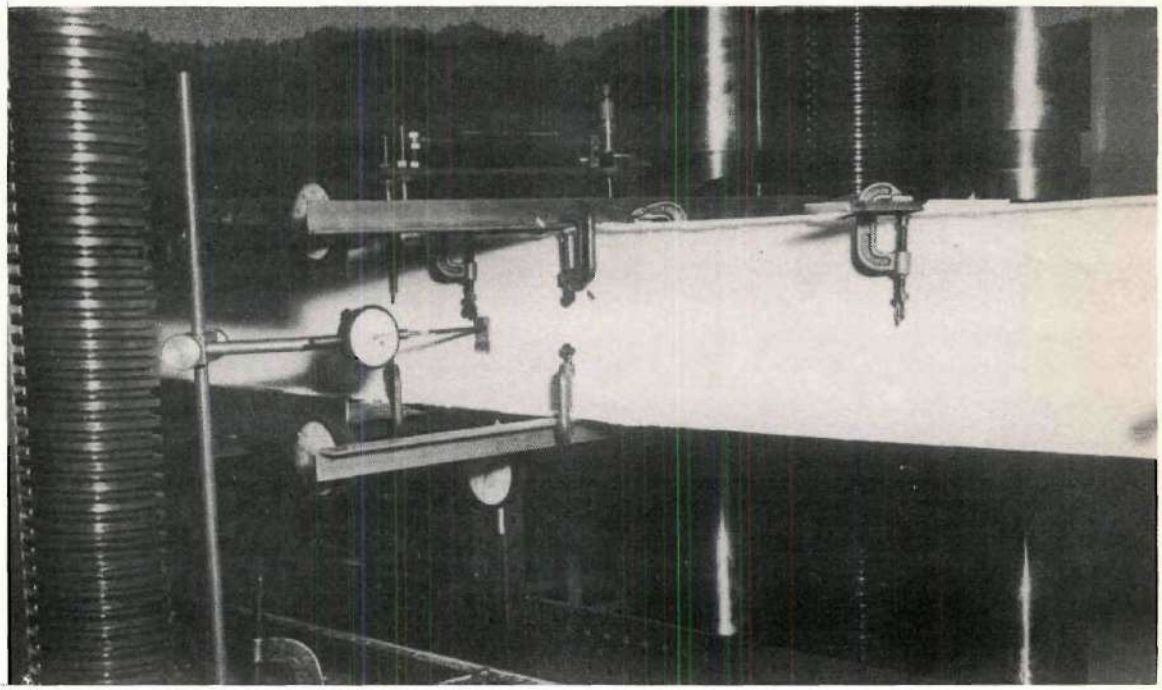

Fig. 6. Typical Centerline Instrumentation for Beam Tests

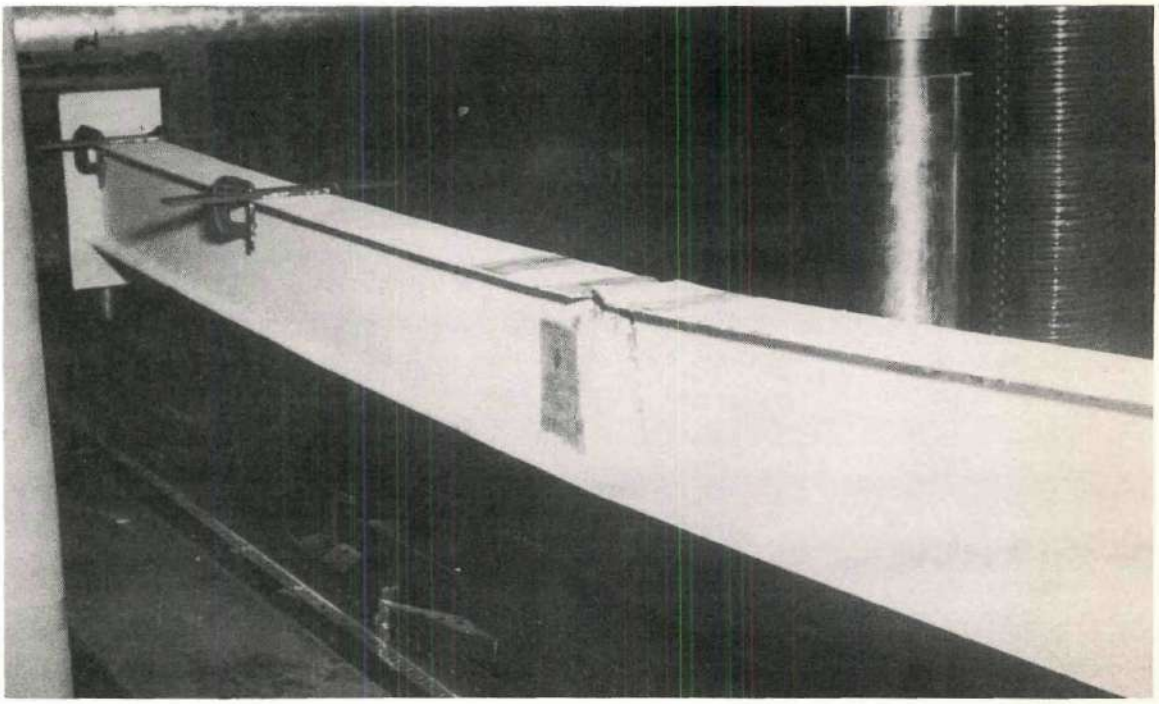

Fig. 7. Local Buckling of Specimen for Test B-3

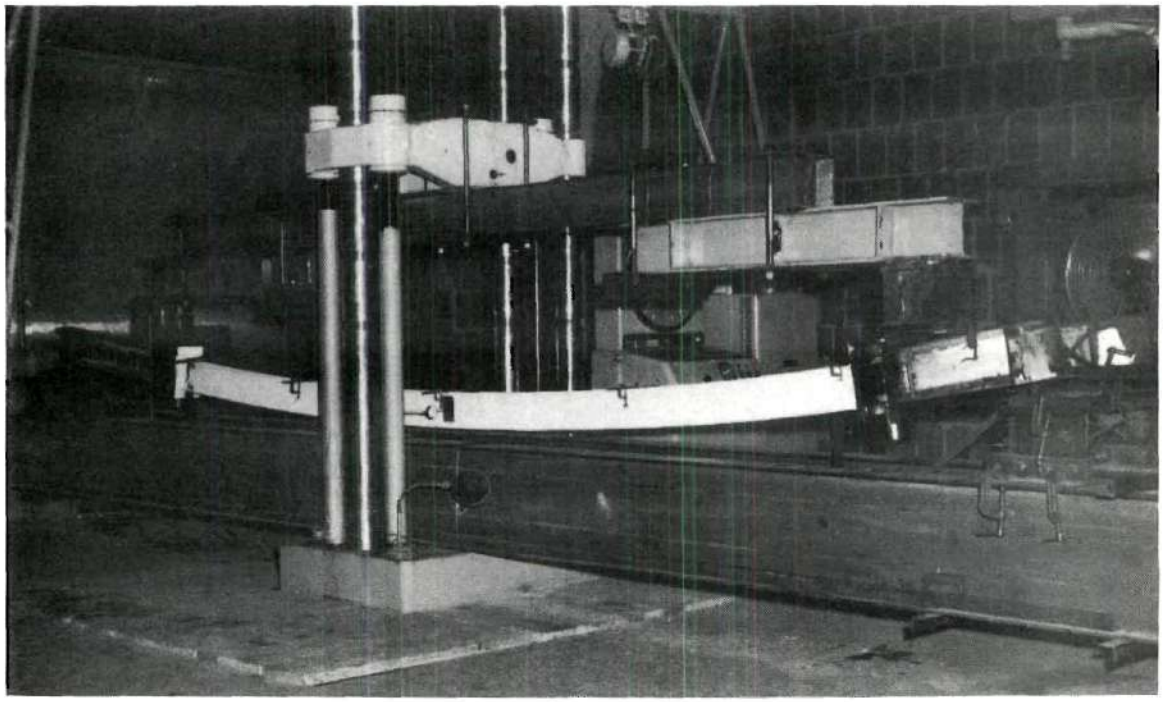

Fig. 8. General View of Test B-4 After Failure

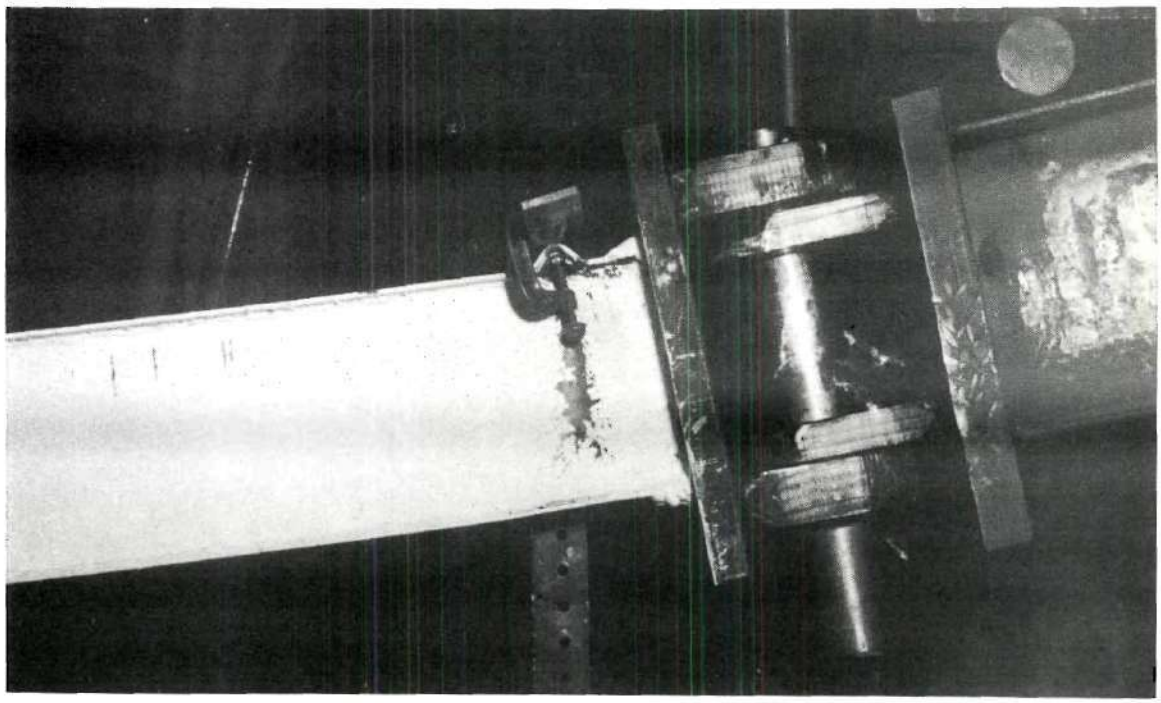

Fig. 9. Local Buckling of Specimen for Test B-4

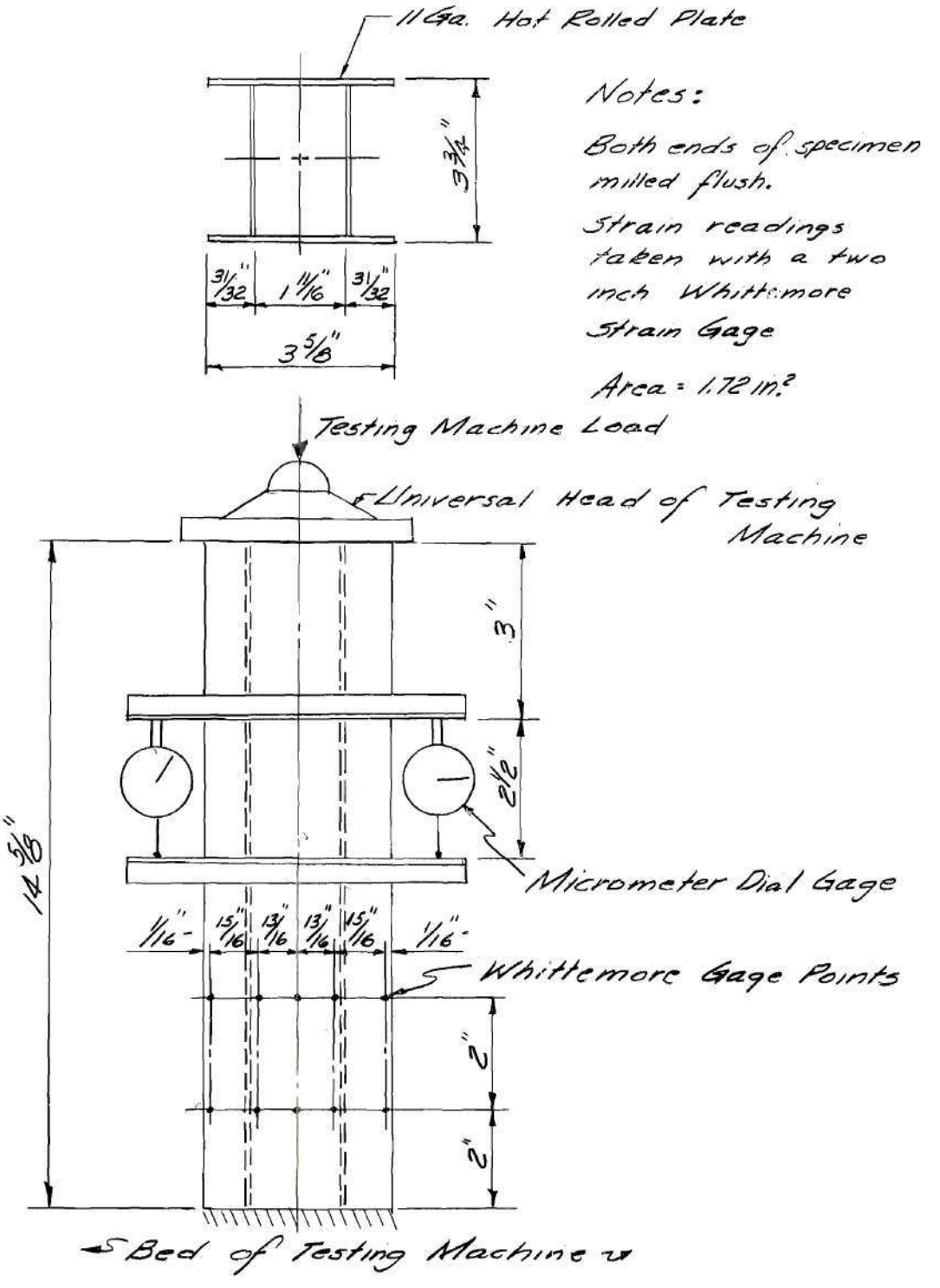

Fig. 10. Test Arrangement and Instrumentation for Compression Test C-1

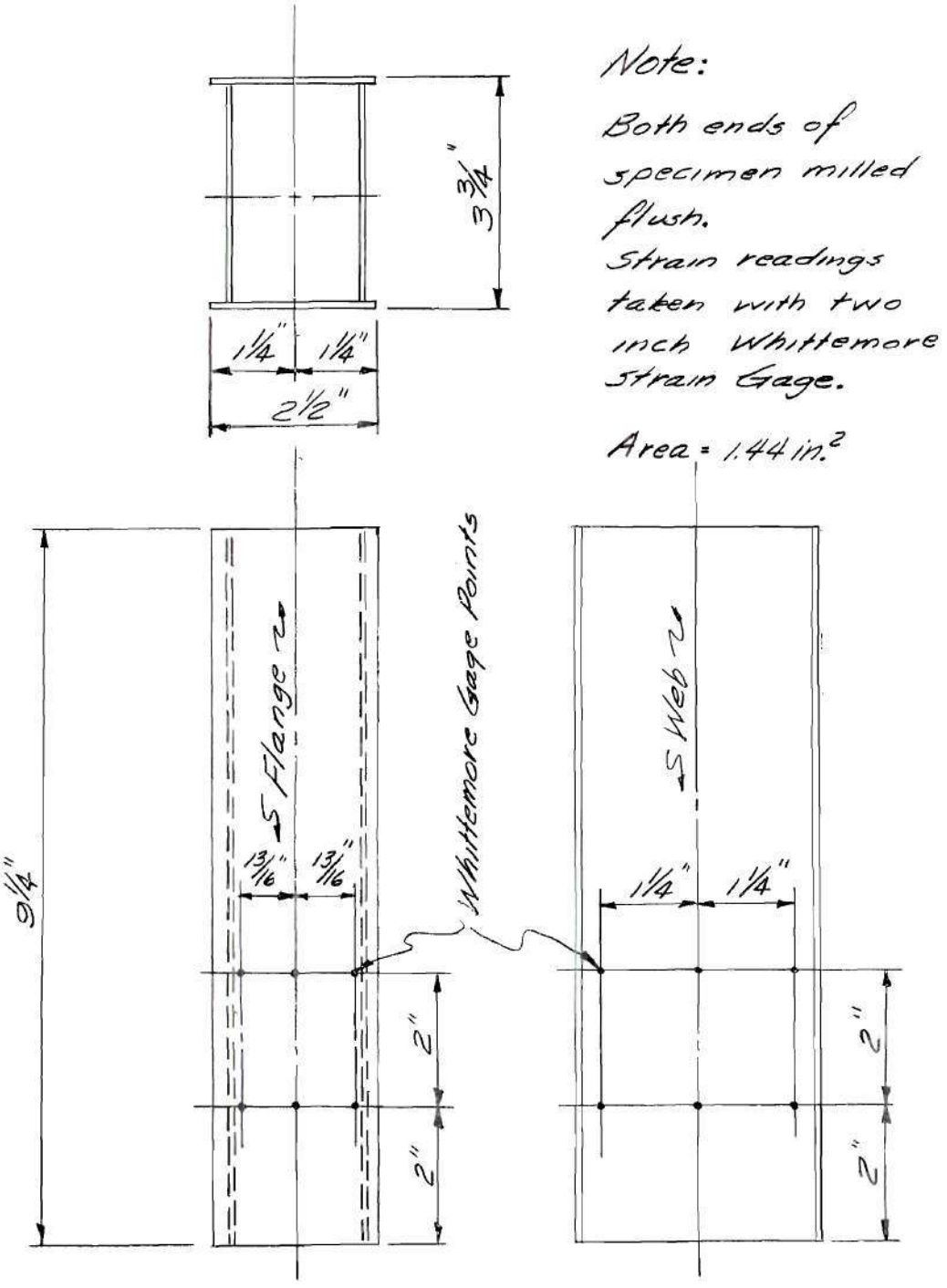

Fig. 11. Detail of Test Specimen for Compression Test C-2

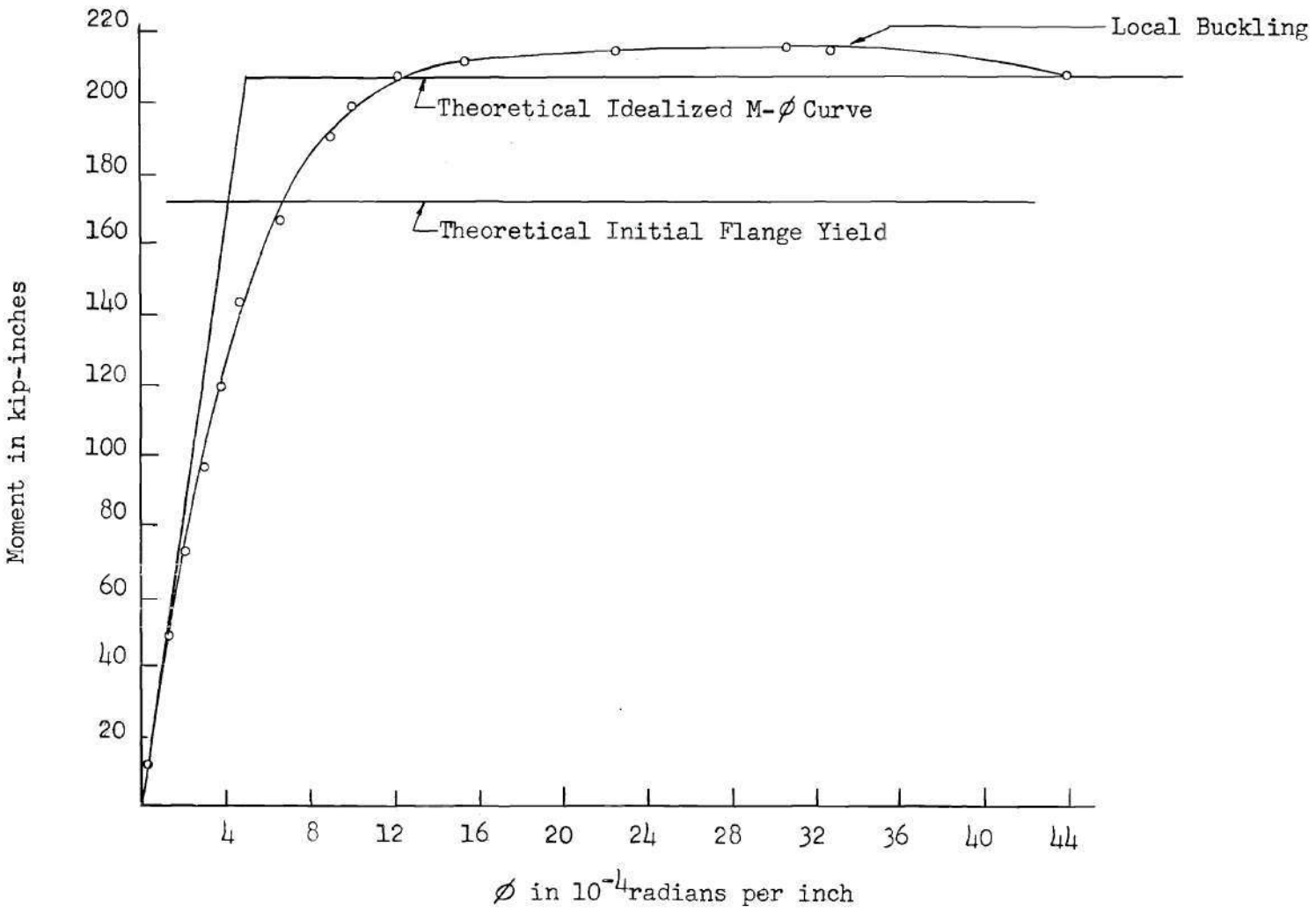

Fig. 12. Moment-Rotation Curve for Test B-1

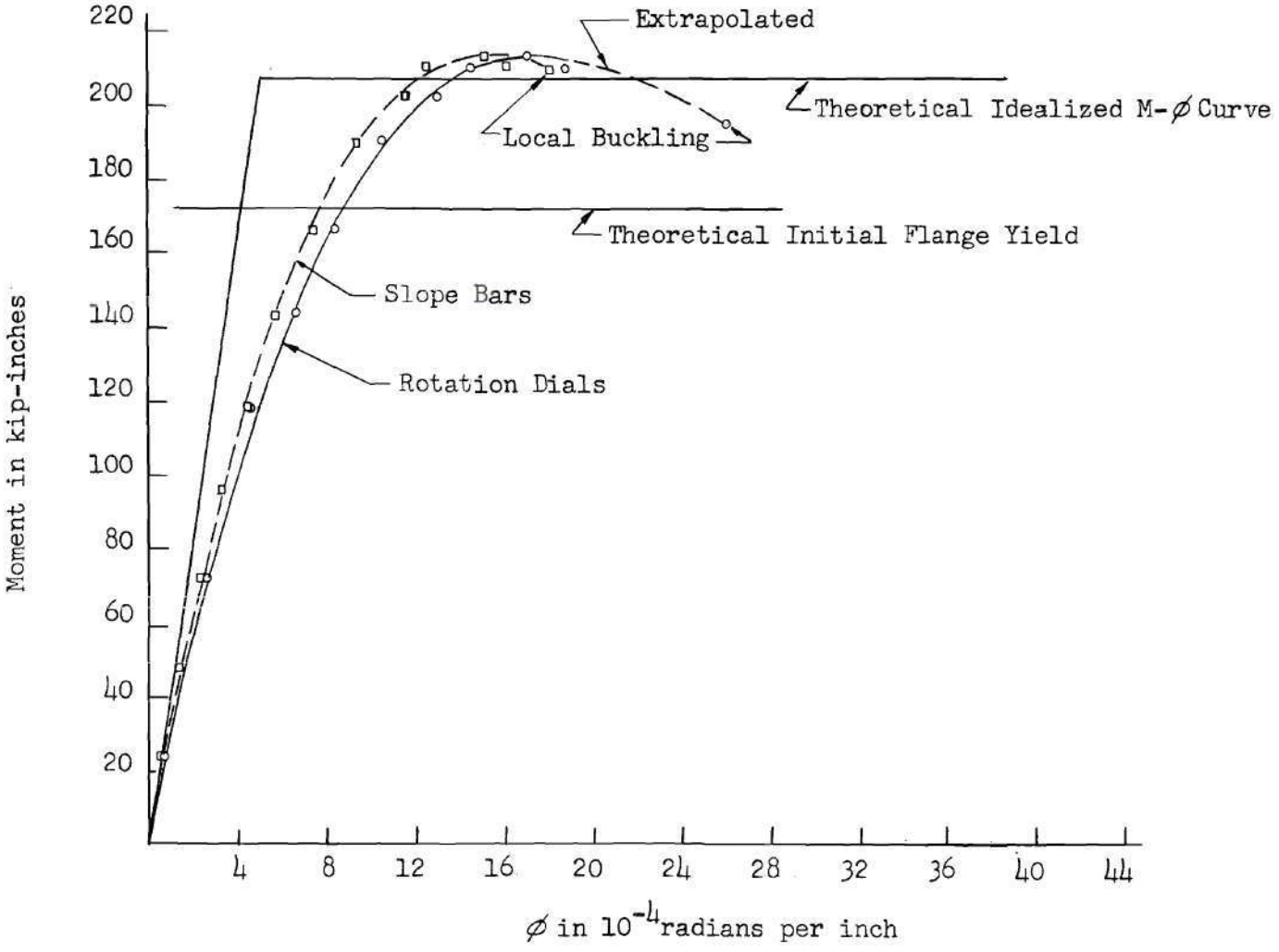

Fig. 13. Moment-Rotation Curve for Test B-2

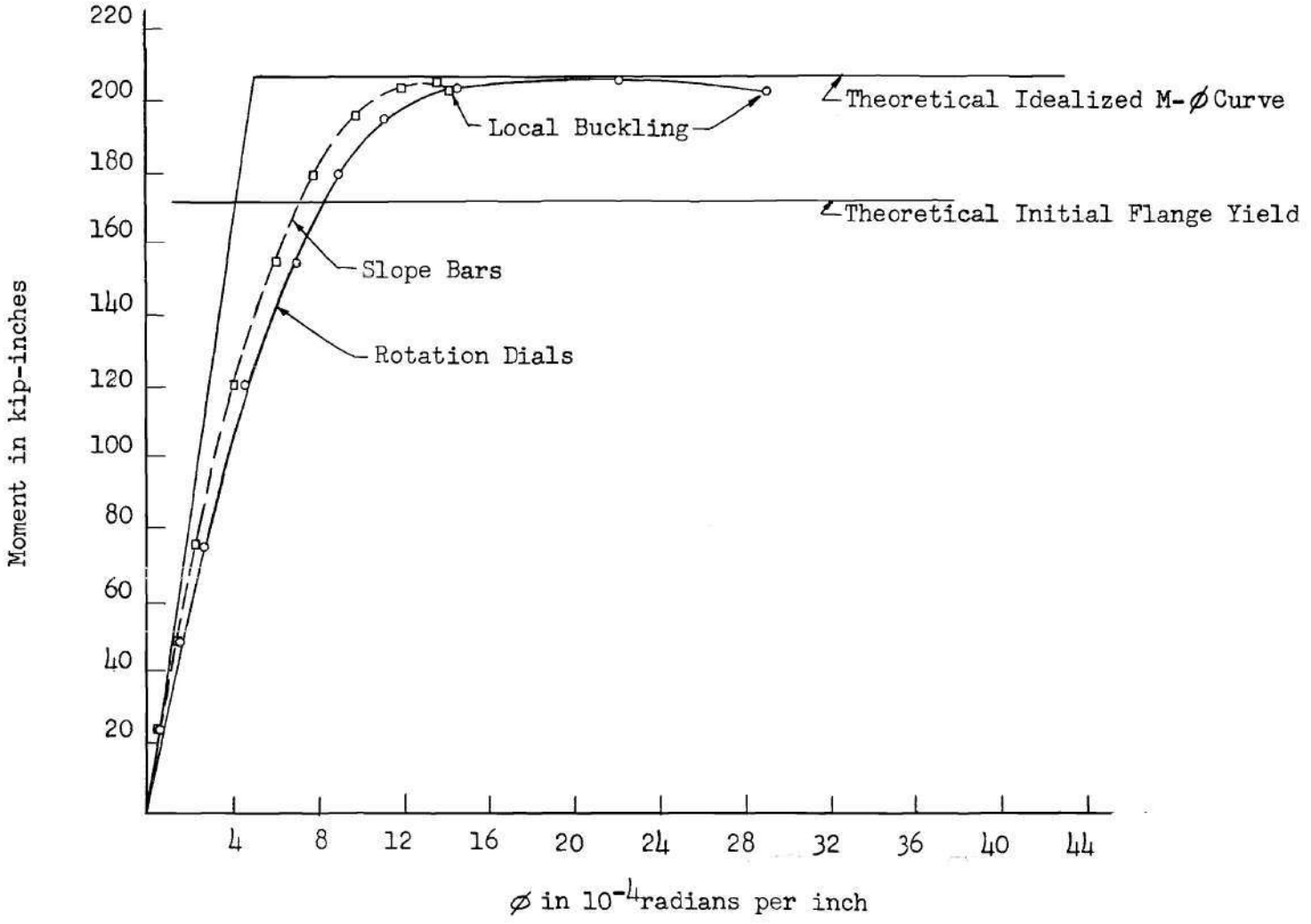

Fig. 14. Moment-Rotation Curve for Test B-3

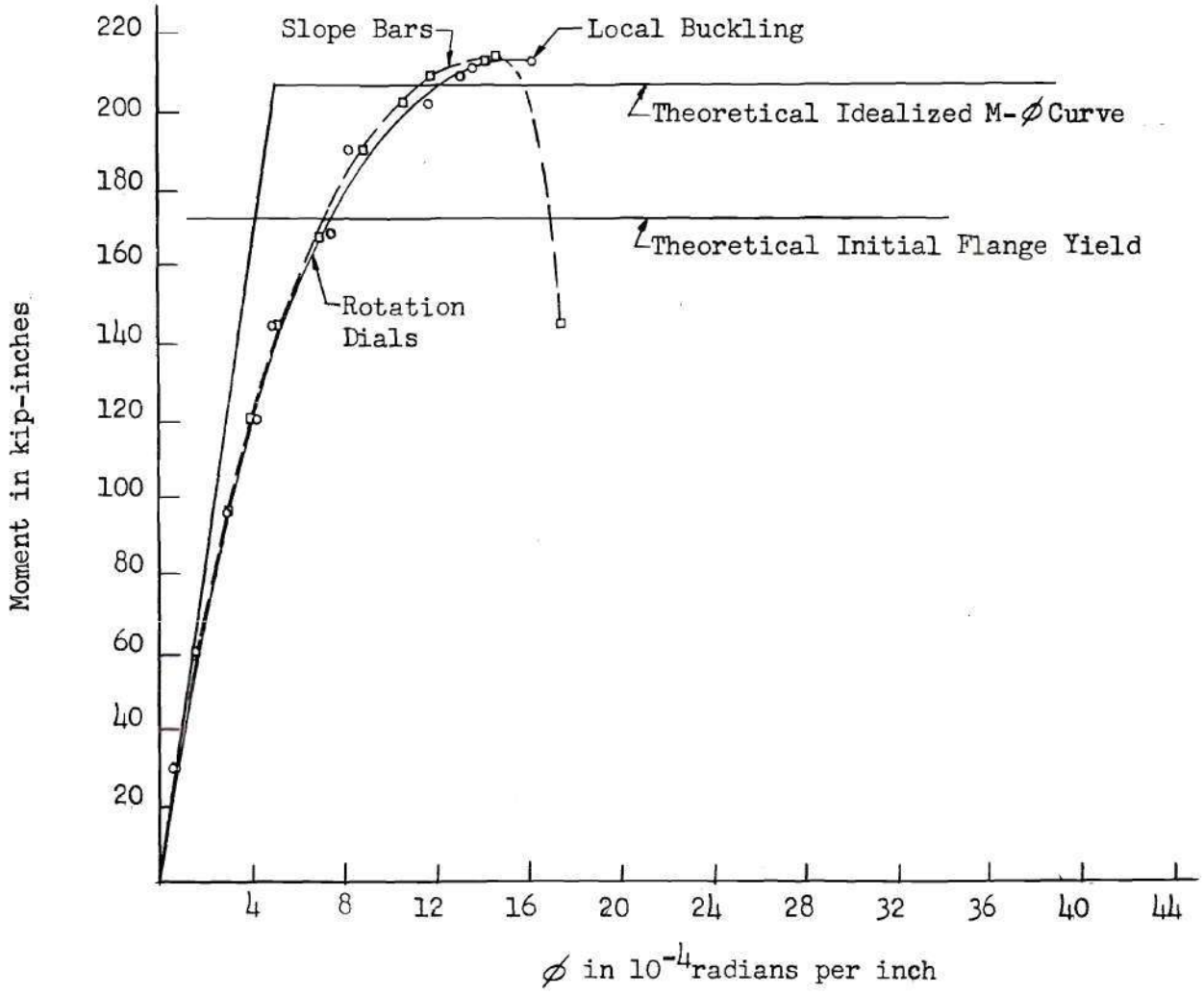

Fig. 15. Moment-Rotation Curve for Test B-4

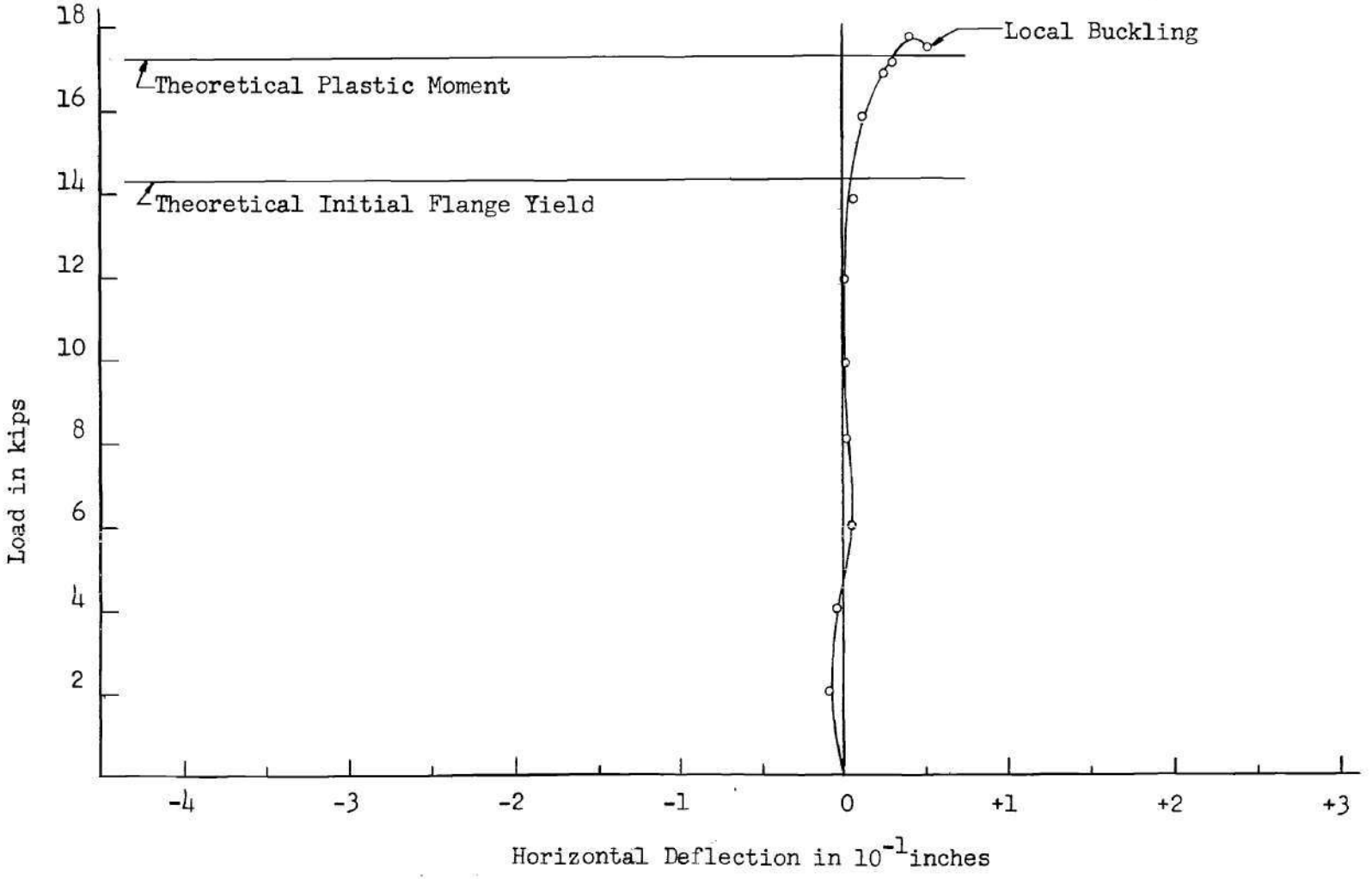

Fig. 16. Horizontal Centerline Deflection for Test B-2

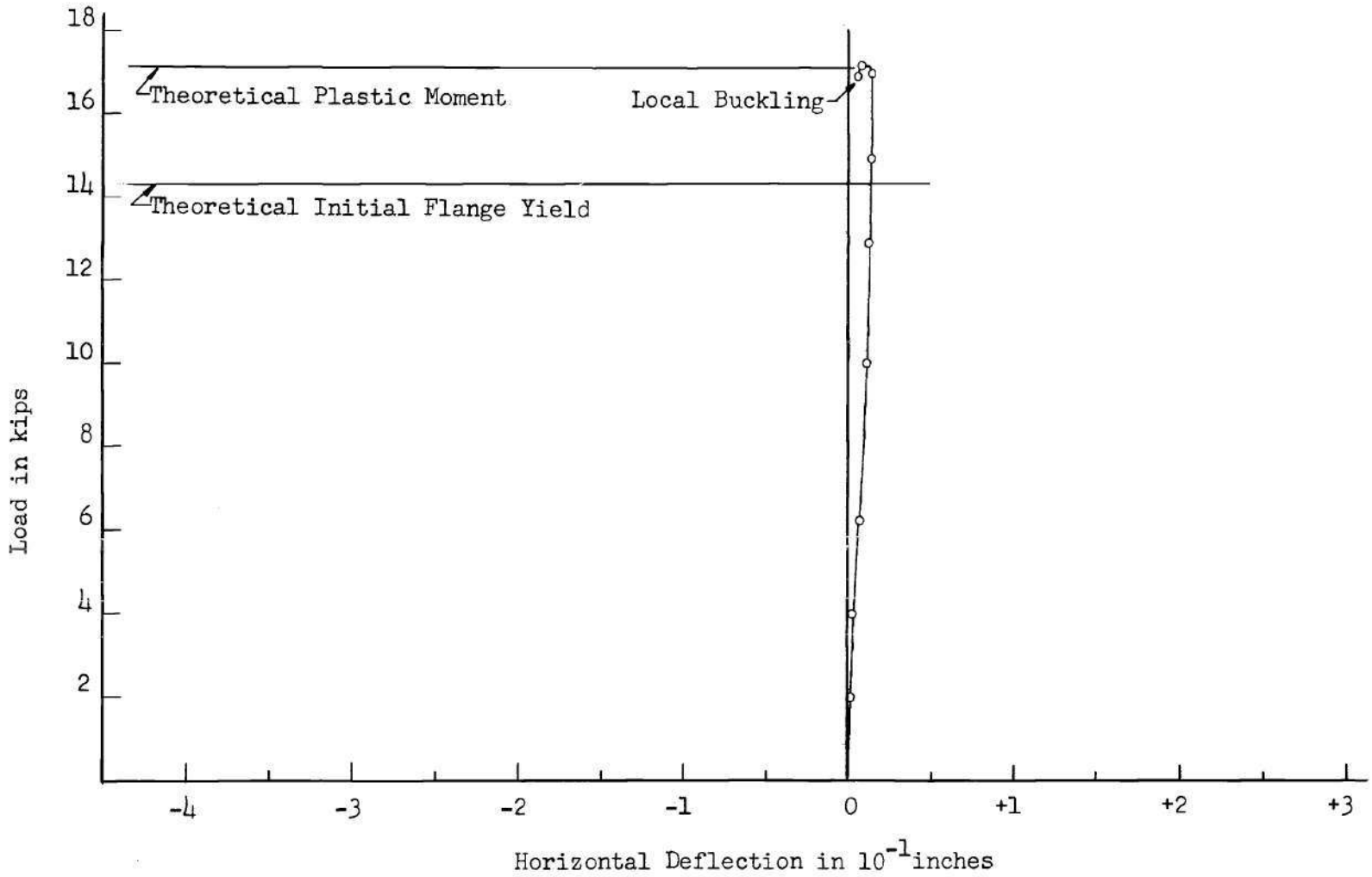

Fig. 17. Horizontal Centerline Deflection for Test B-3

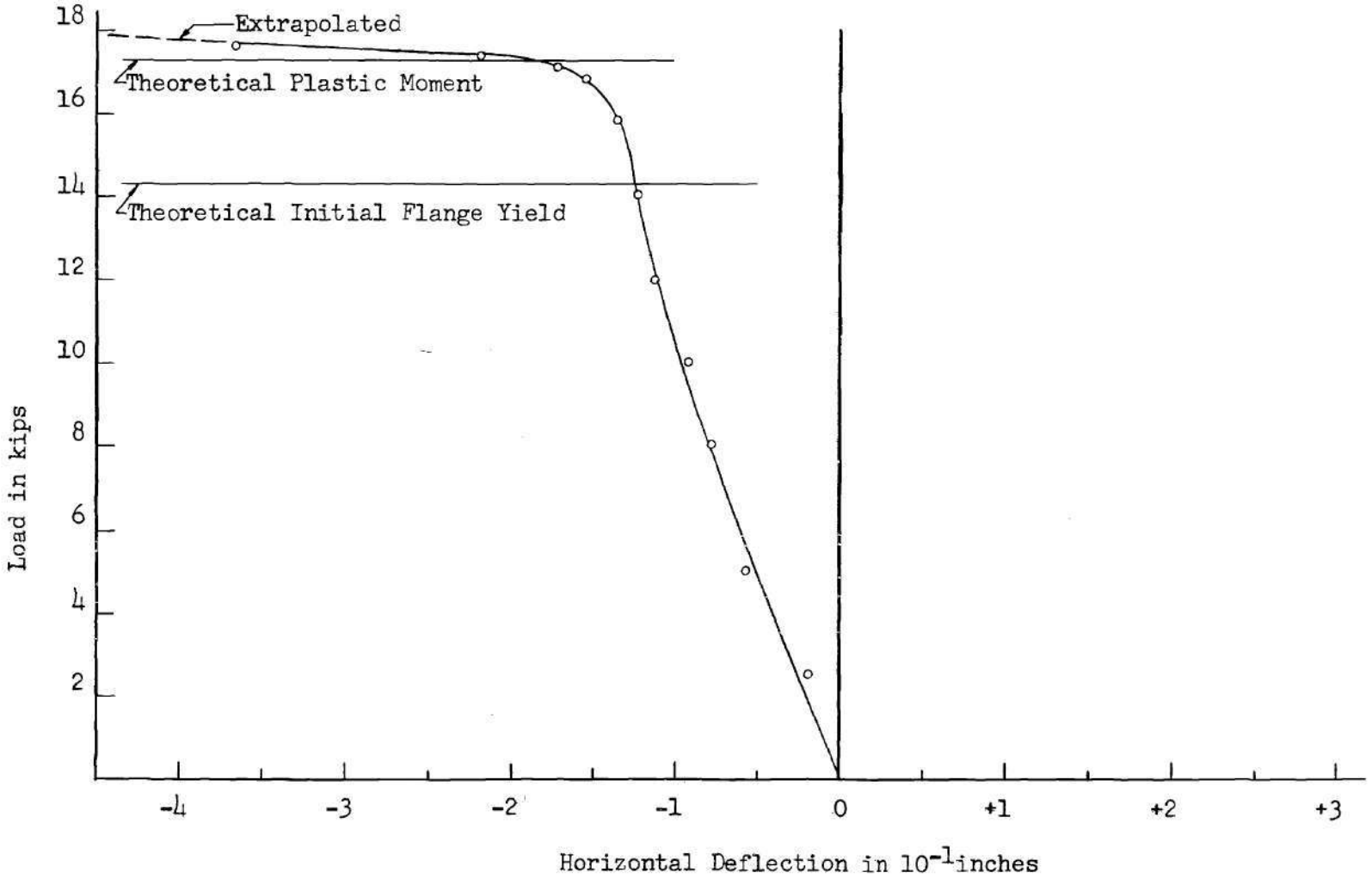

Fig. 18. Horizontal Centerline Deflection for Test B-4

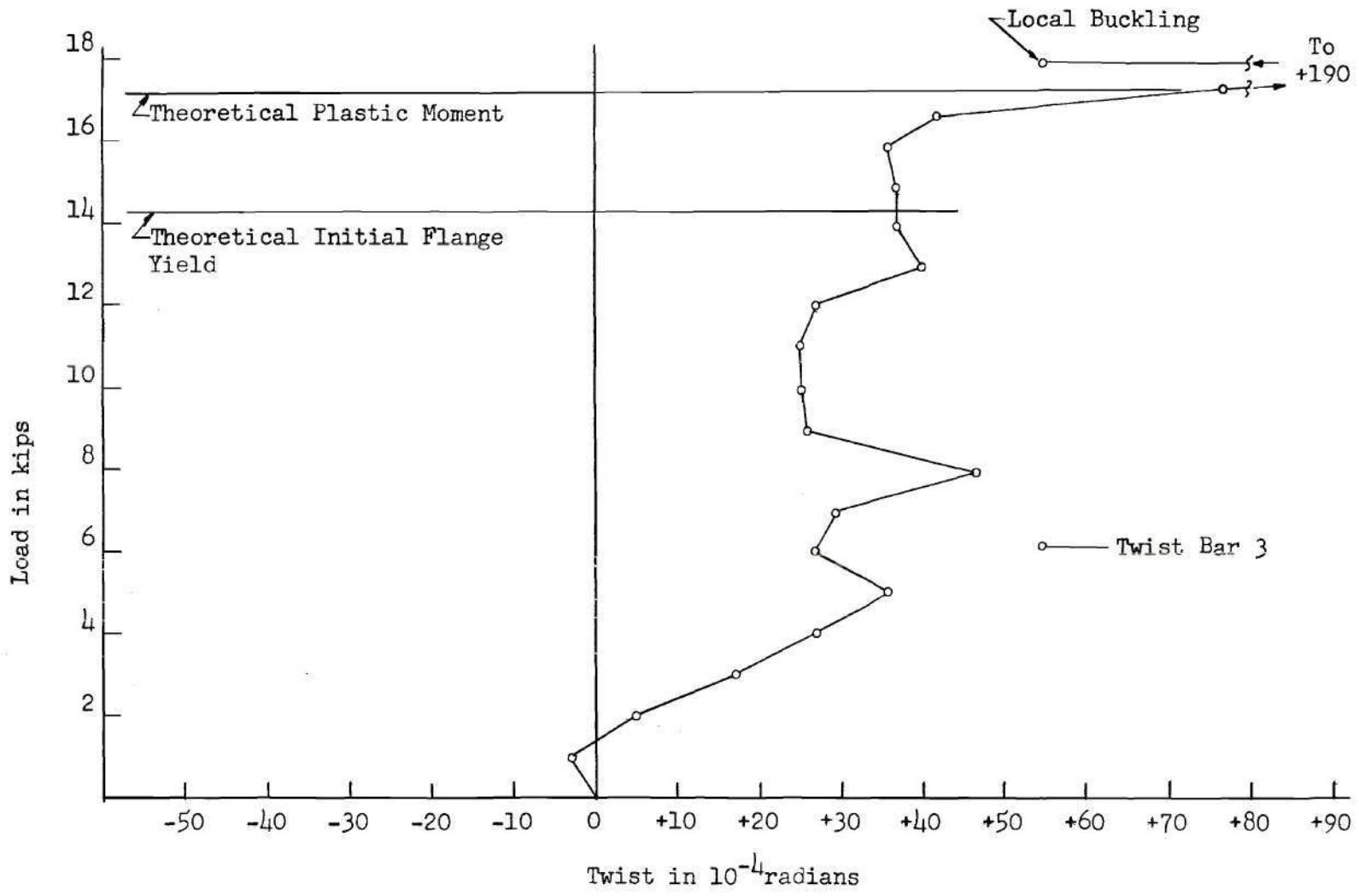

Fig. 19. Twist Curve for Test B-1

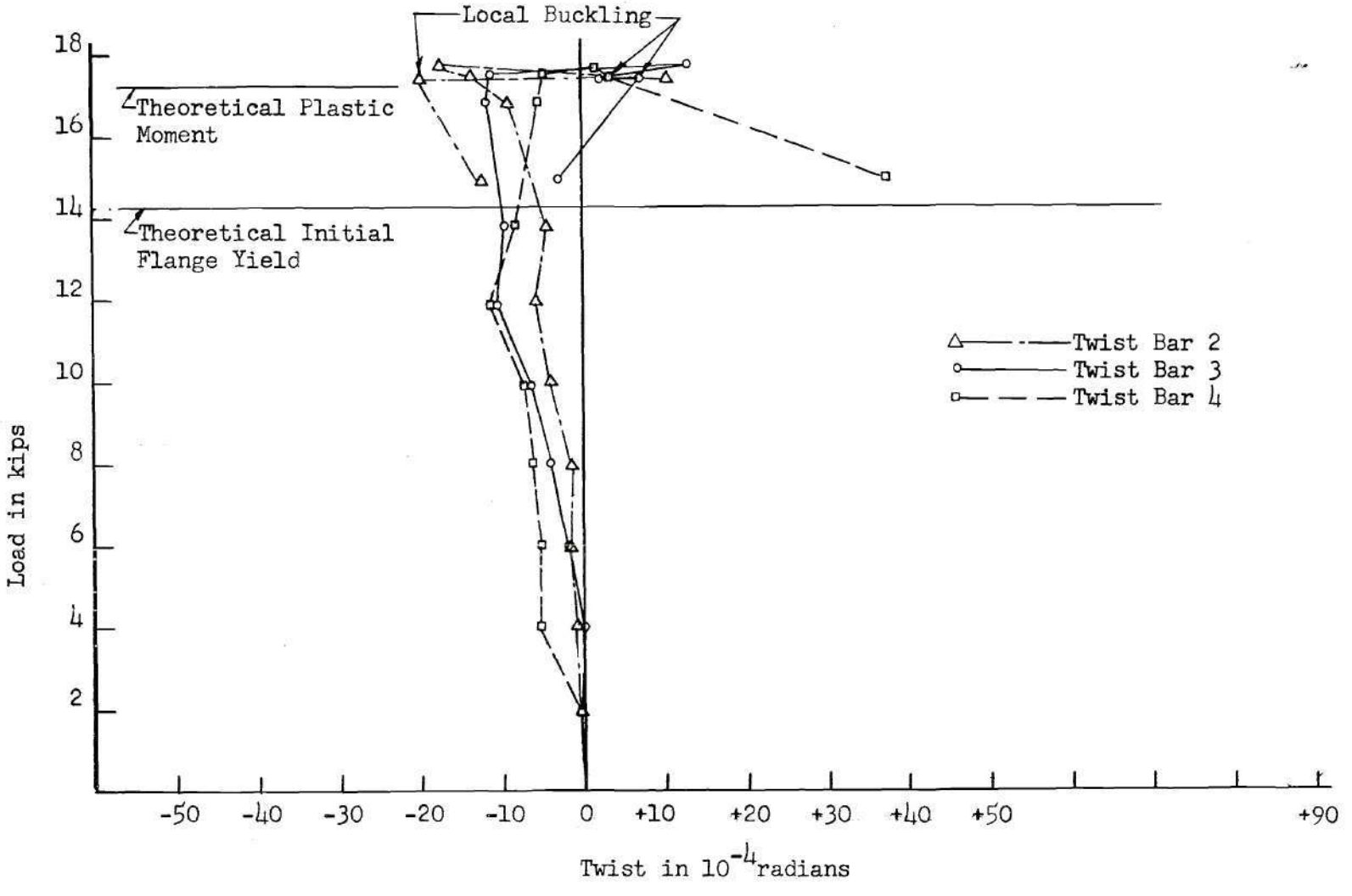

Fig. 20. Twist Curve for Test B-2

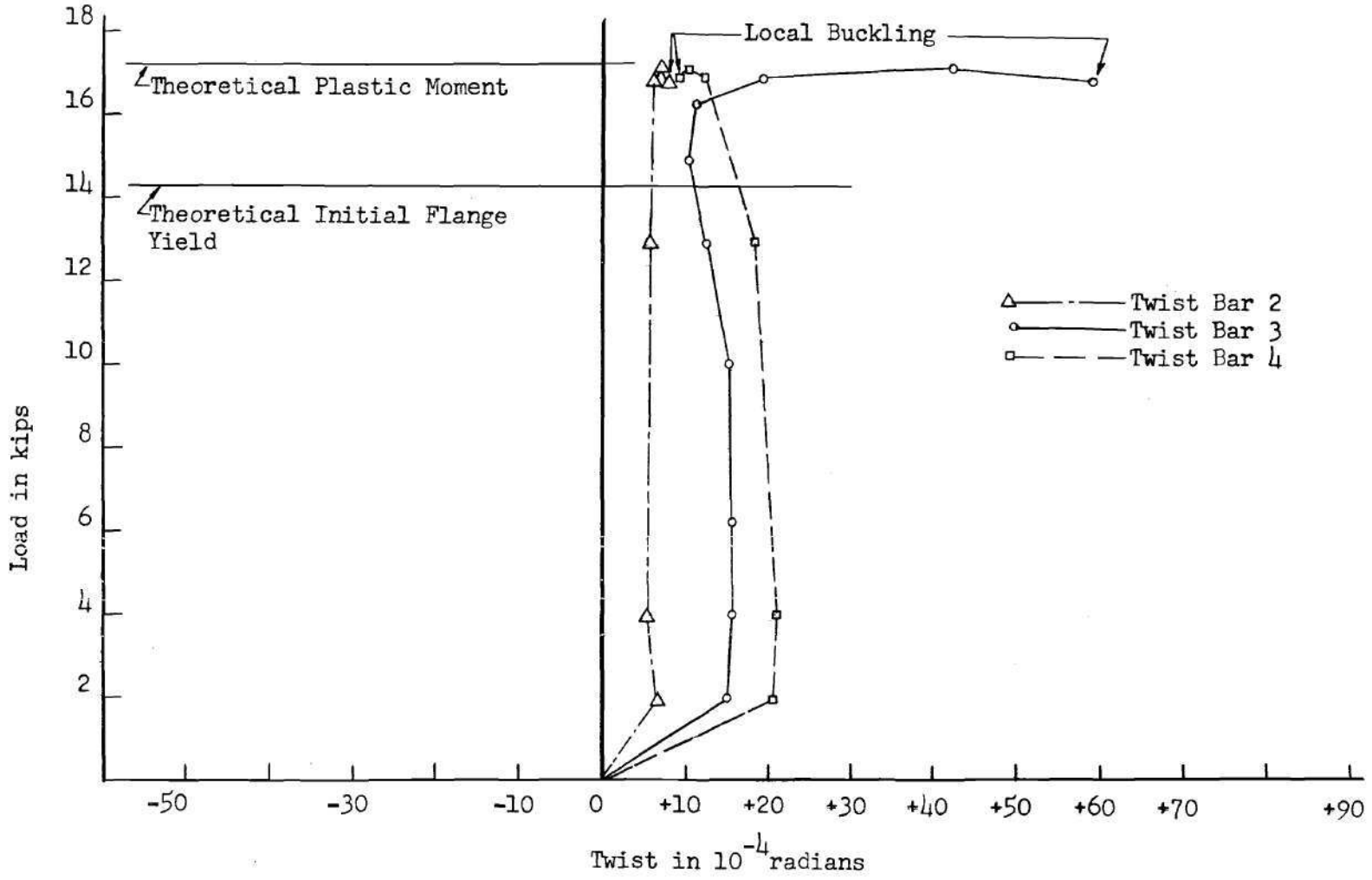

Fig. 21. Twist Curve for Test B-3

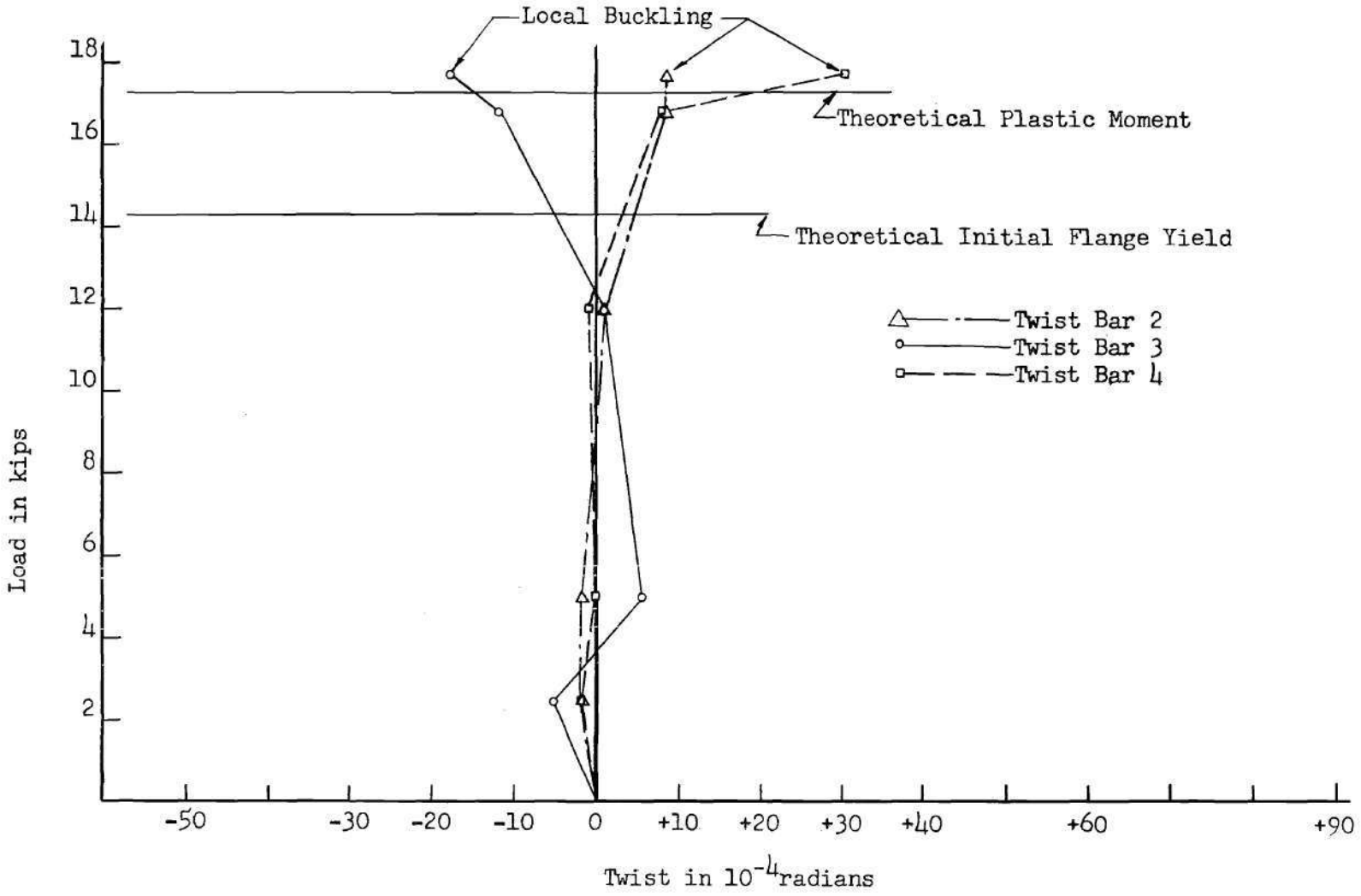

Fig. 22. Twist Curve for Test B-4

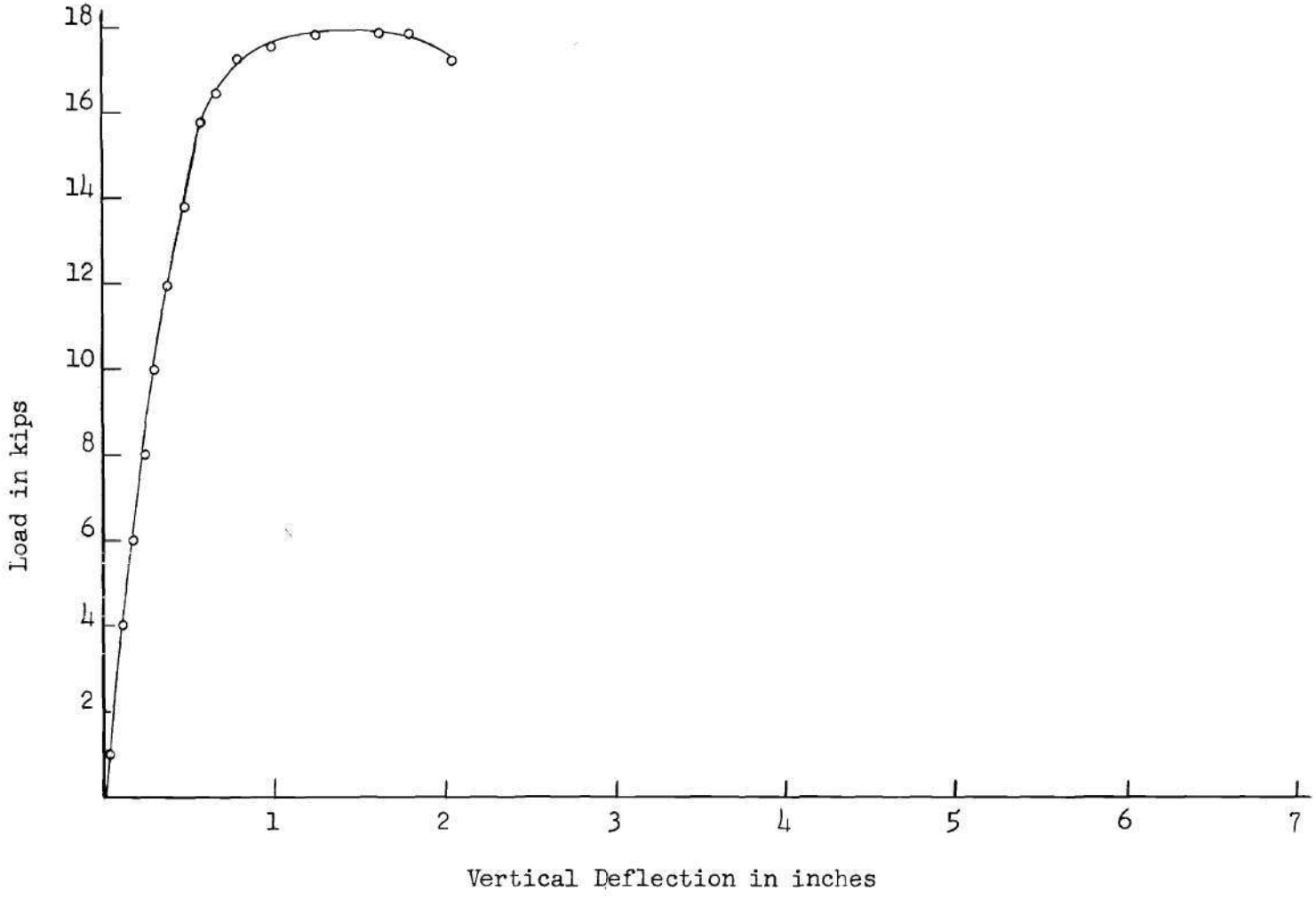

Fig. 23. Vertical Centerline Deflection for Test B-1

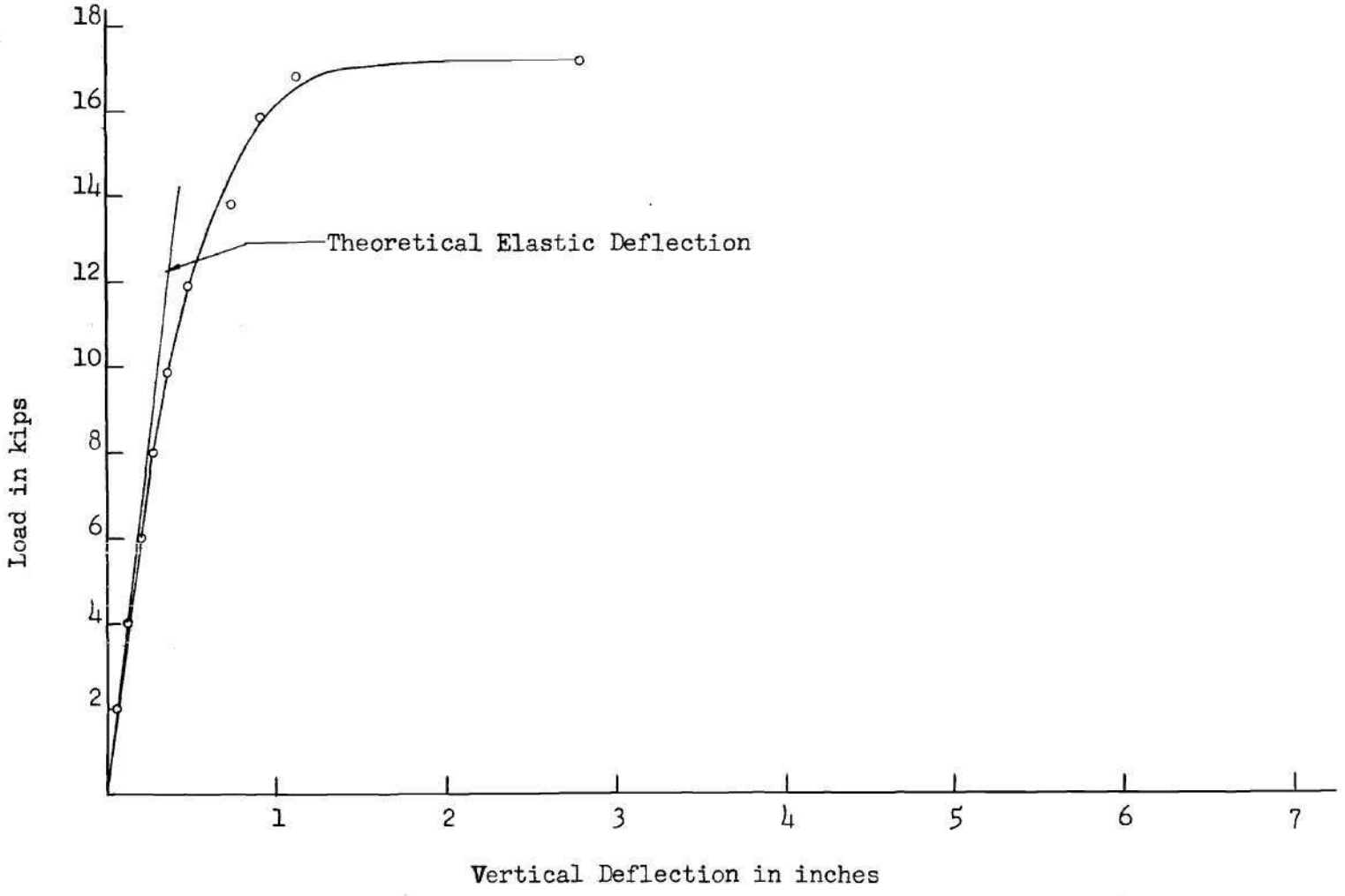

Fig. 24. Vertical Centerline Deflection for Test B-2

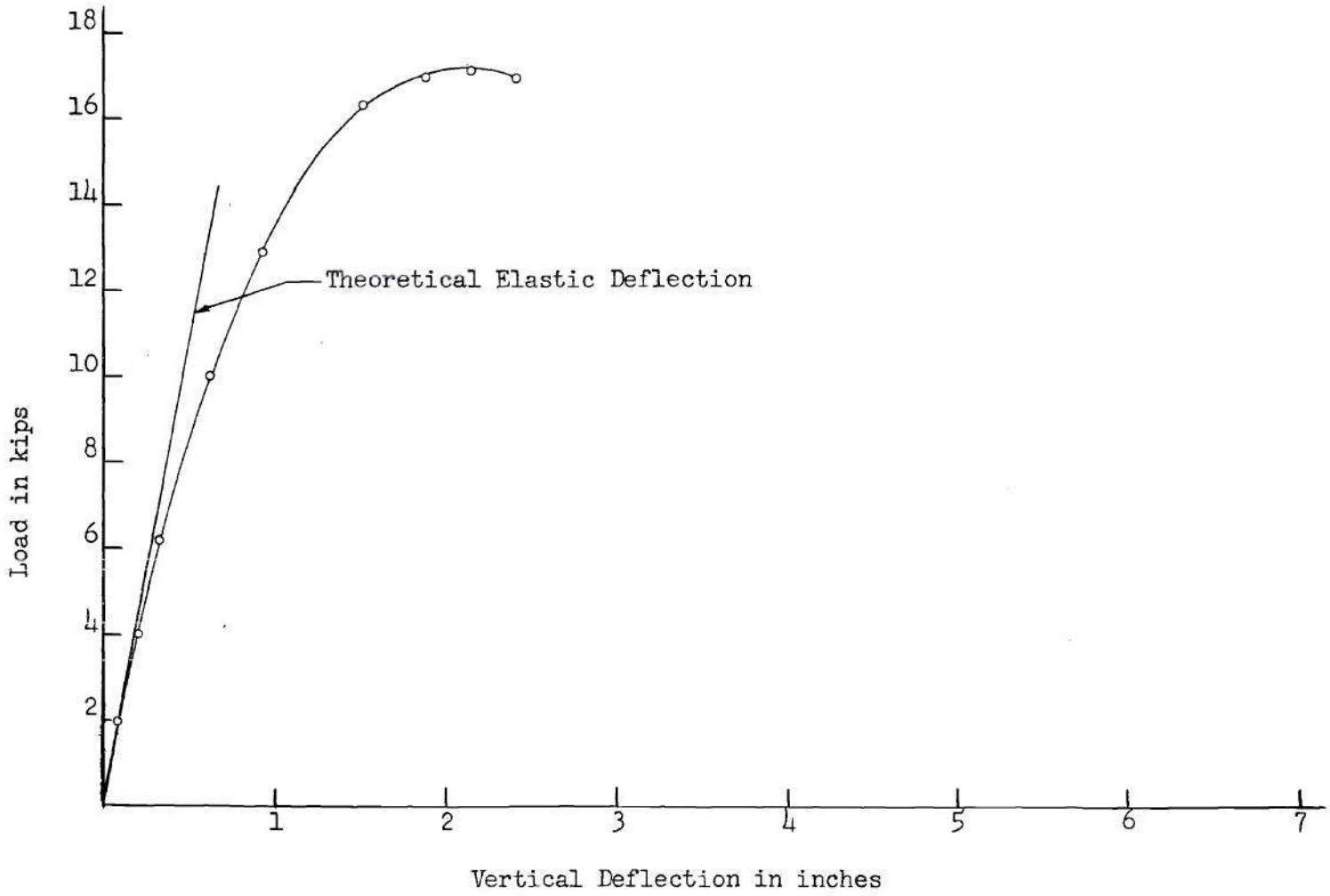

Fig. 25. Vertical Centerline Deflection for Test B-3

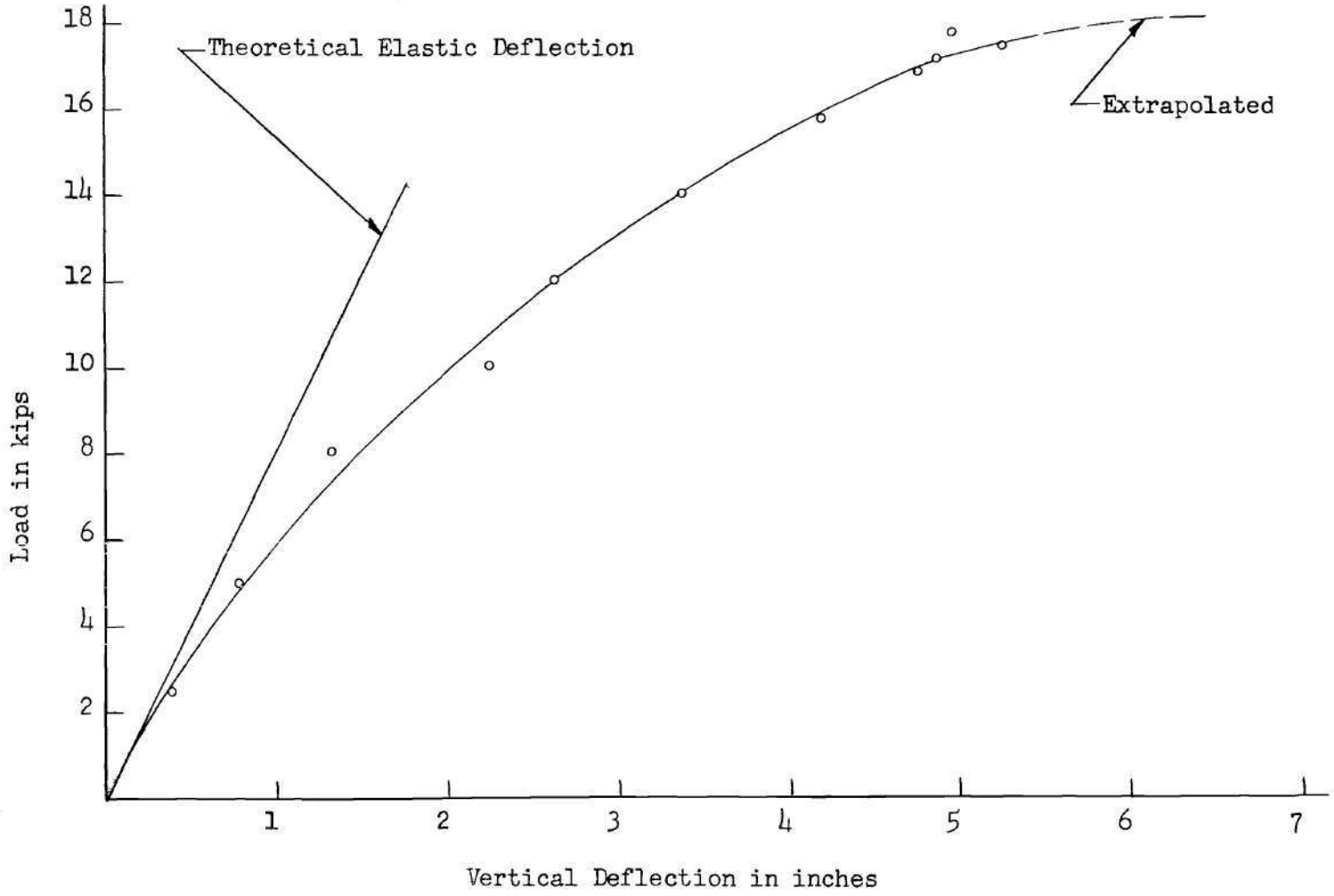

Fig. 26. Vertical Centerline Deflection for Test B-4

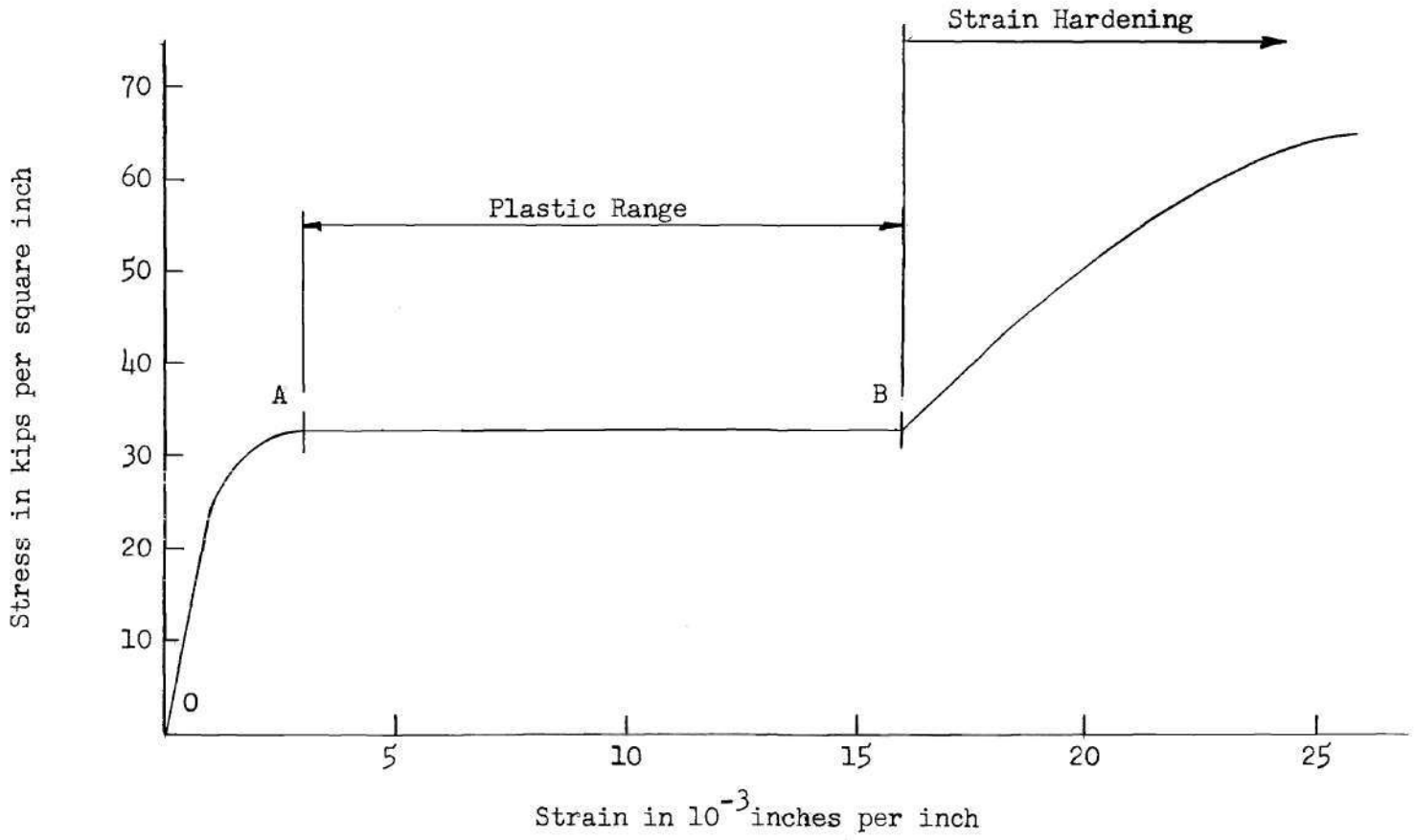

Fig. 27. Typical Stress-Strain Curve for Mild Structural Steel

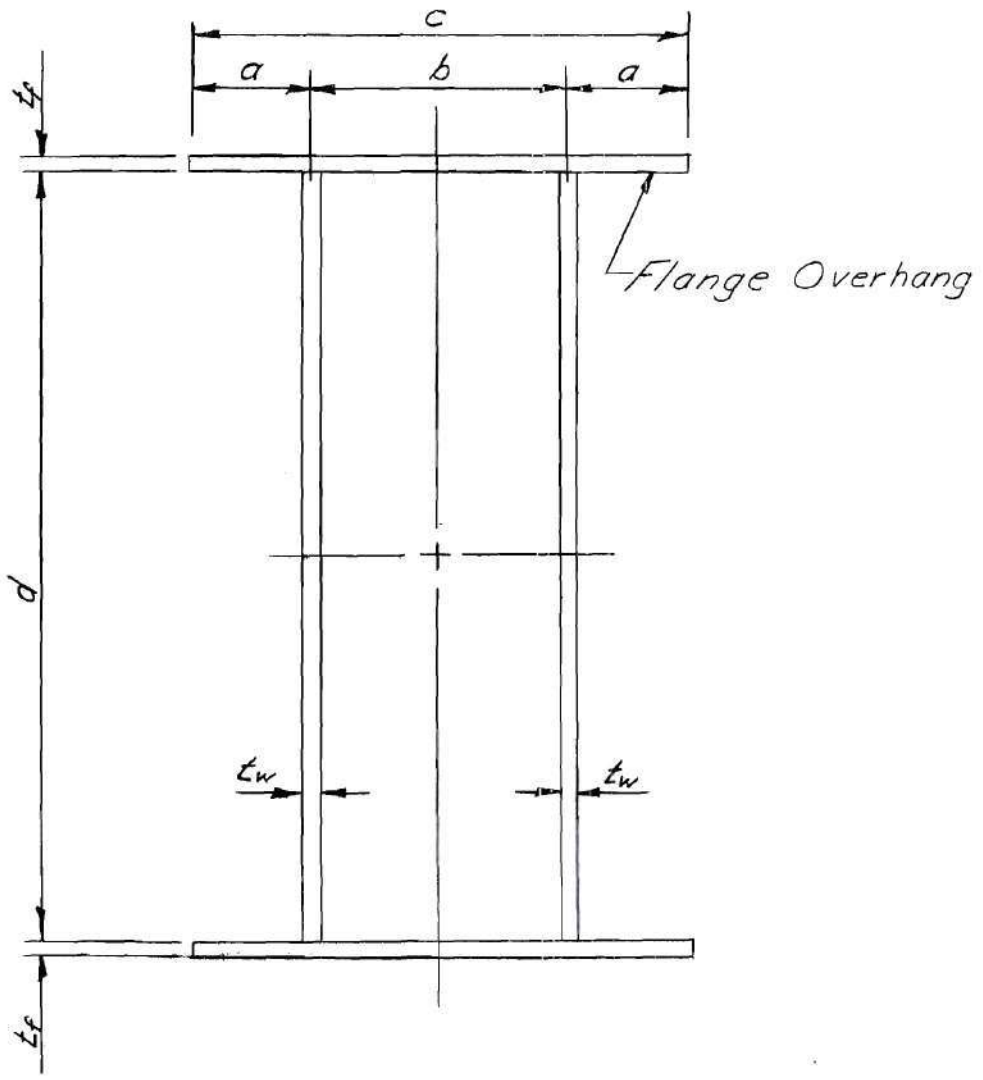

Fig. 28. Notation for General Box Section

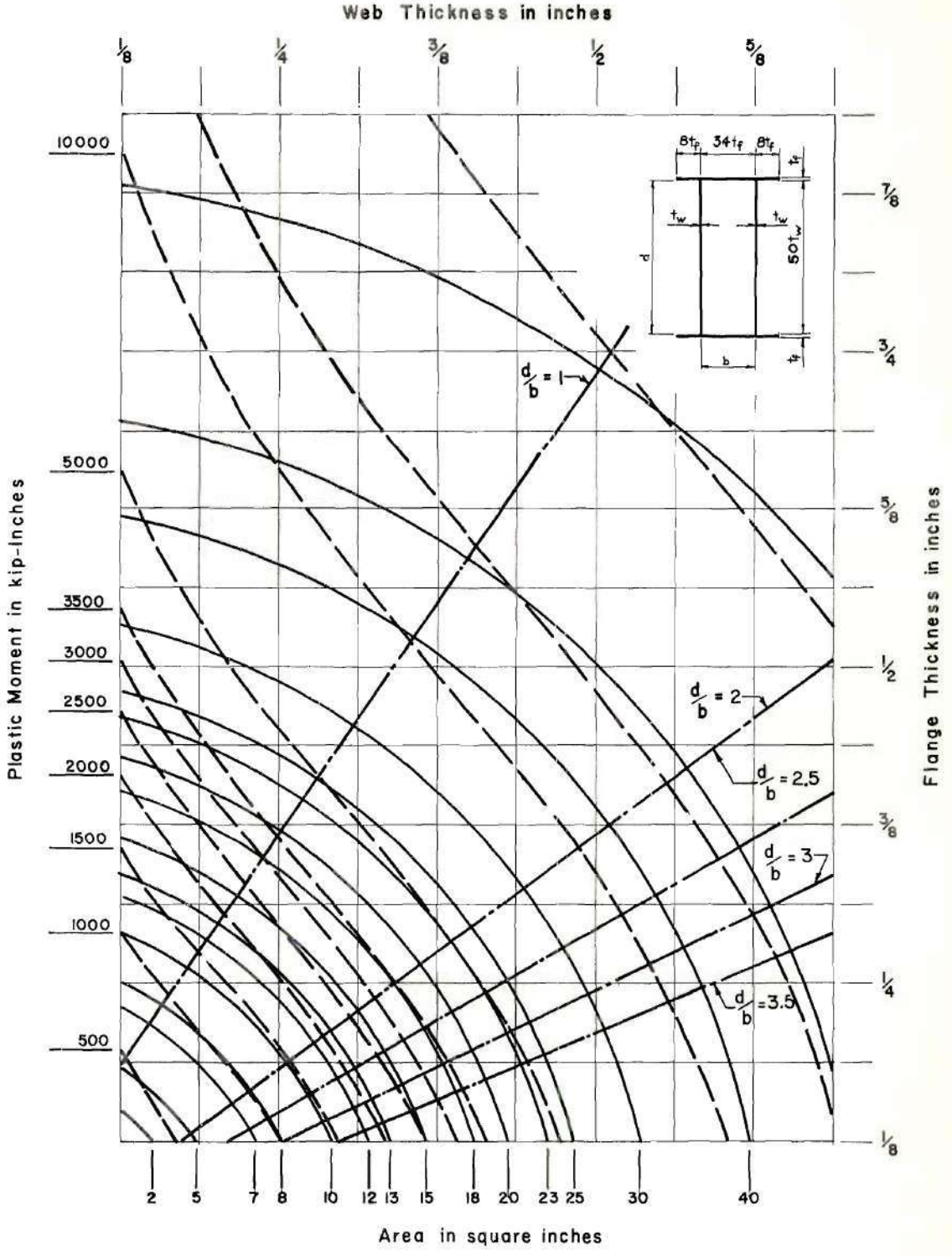

Fig. 29. Chart for Determination of Most Economical Box Section

APPENDIX C

TABLES

Table 1. Instrumentation Dimensions

Test Number	L	m	n	p	r	s	v	x	z
B-1	31.5	- -	- -	- -	- -	- -	- -	7.13	10.50
B-2	93.5	19.5	21.3	21.5	19.5	41.0	41.0	7.53	10.56
B-3	118.5	24.0	28.5	27.5	24.1	53.5	53.5	7.38	10.63
B-4	187.5	42.2	43.5	45.8	42.5	88.0	88.0	7.50	10.63

Note: All dimensions are in inches.
The above dimensions refer to Fig. 4.

Table 2. Summary of Beam Test Results

Test Number	L in inches	ϕ_f x10^4 rad/in	ϕ_f / ϕ_y	Observed Mp in kip-inches	Theoretical Mp in kip-inches
B-1	31.5	33.0	8.13	215	207.3
B-2	93.5	22.0	5.42	212	207.3
B-3	118.5	22.0	5.42	210	207.3
B-4	187.5	16.2	4.00	212	207.3

Table 3. Summary of Compression Test Results

Test Number	ϵ_f (Flange Whittemore Readings)	ϵ_f (Flange Dial Readings)	ϵ_f (Web Whittemore Readings)	ϵ_f (Head Dial Reading)	Theoretical ϵ_y	ϵ_f/ϵ_y (Average)	Failure Load in kips
C-1	3.52	3.56	—	4.75	1.32	2.98	75.0
C-2	5.30	—	4.89	—	1.32	3.86	64.8

Note: All the above figures are x 10^3in/in except where noted.

Table 4. Results of Coupon Tension Tests

Sheet Number	Coupon Number	σ_{yu} in ksi	σ_y in ksi	σ_{ult} in ksi	ϵ_y x10^{3}in/in	ϵ_{st} x10^{3}in/in	E x10^{-3}ksi	Est in ksi
1	15	40.9	38.2	49.7	1.65	26.1	26.0	213
2	1	31.6	30.0	44.0	1.65	17.0	24.2	206
2	3	36.8	34.6	48.2	1.65	21.2	31.3	211
2	5	39.7	36.6	49.7	1.55	25.5	28.1	211
2	7	40.2	38.4	50.6	—	26.0	24.8	211
2	15	41.0	38.2	50.5	1.50	25.9	28.0	210
2	23	41.5	38.0	49.7	1.65	25.3	31.3	206
2	25	40.2	38.0	51.0	1.65	25.1	28.1	206
2	27	39.2	37.0	49.4	1.65	25.1	27.5	203
2	29	37.6	35.5	49.3	1.50	23.6	30.0	205
2	31	34.3	32.6	46.0	1.40	21.5	28.0	205
4	15	41.5	38.4	50.0	1.65	31.8	28.6	--

Note: The above coupons were tested with an Olsen "Super L" Hydraulic Universal Testing Machine.

Table 5. Results of Coupon Tension Tests

Sheet Number	Coupon Number	σ_{yu} in ksi	σ_{y} in ksi	σ_{ult} in ksi	ϵ_{y} $x10^{3}$ in/in	ϵ_{st} $x10^{3}$ in/in	E $x10^{-3}$ ksi	Est in ksi
1	17	40.6	40.0	49.3	1.40	20.0	31.3	222
2	13	—	39.4	48.5	1.25	22.0	29.4	286

Note: The above coupons were tested with an Olsen Electomatic Screw Powered Universal Testing Machine.

Table 6. Results of Chemical Analysis of Material Used

Element	o/o
Carbon	0.036
Sulfur	0.011
Phosphorous	0.009
Manganese	0.370
Silicon	0.000
Copper	0.000

Table 7. Results of Theoretical Calculations for Compression Tests

Test Number	Flange Overhang ϵ_f (Simply Supported Edge, Eq. 1)	Flange Overhang ϵ_f (Fixed Edge, Eq. 2)	Webs ϵ_f (Simply Supported Edge, Eq. 3	Webs ϵ_f (Fixed Edge, Eq. 4)
C-1	2.16	2.83	2.36	2.63
C-2	--	--	2.98	3.39

Note: All the above figures are $x10^3$ in/in.

Table 8. Results of Theoretical Calculations of Width to Thickness Ratios Required for the Material of this Study

Flange Overhang a/t_f Simply Supported Edge, Eq. 8.	Flange Overhang a/t_f Fixed Edge, Eq. 9.	Webs d/t_w Simply Supported Edges, Eq. 10.	Webs d/t_w Fixed Edges, Eq. 11.
5.68	9.08	19.5	26.2

BIBLIOGRAPHY

LITERATURE CITED

(1) Beedle, Lynn S., Bruno Thurlimann, and Robert L. Ketter, Plastic Design in Structural Steel, Lecture Notes, Lehigh University and American Institute of Steel Construction, Bethlehem, Pennsylvania, Sept. 1955, Section 10.

(2) Thurlimann, Bruno and G. Haaijer, Local Buckling of Wide-Flange Shapes, Unpublished Progress Report, Welded Continuous Frames and Their Components, Lehigh University, December, 1954.

(3) Thurlimann, Bruno and G. Haaijer, Buckling of Steel Angles in the Plastic Range, Unpublished Progress Report, Welded Continuous Frames and Their Components, Lehigh University, August 15, 1953.

(4) Timoshenko, S., Theory of Elastic Stability, McGraw-Hill Book Co., Inc., New York, New York, 1936, pp. 327-342.

(5) Bleich, F., Buckling Strength of Metal Structures, McGraw-Hill Book Co., Inc., New York, New York, 1952, p. 330.

(6) Timoshenko, op. cit., pp. 239-242.

OTHER REFERENCES

(1) Steel Construction Manual, Fifth edition, New York, New York: American Institute of Steel Construction, 1955.